The effects of Antarctic alteration and sample heterogeneity on Sm-Nd and Lu-Hf systematics in H chondrites

Maeda, Ryoga; Goderis, Steven; Debaille, Vinciane; Pourkhorsandi, Hamed; Hublet, Geneviève; Claeys, Philippe

Published in:
Geochimica et Cosmochimica Acta

DOI:
10.1016/j.gca.2021.05.005

Publication date:
2021

Citation for published version (APA):
Maeda, R., Goderis, S., Debaille, V., Pourkhorsandi, H., Hublet, G., & Claeys, P. (2021). The effects of Antarctic alteration and sample heterogeneity on Sm-Nd and Lu-Hf systematics in H chondrites. *Geochimica et Cosmochimica Acta*, *305*, 106-129. https://doi.org/10.1016/j.gca.2021.05.005

The effects of Antarctic alteration and sample heterogeneity on Sm-Nd and Lu-Hf systematics in H chondrites

Ryoga Maeda[a,b,*], Steven Goderis[a], Vinciane Debaille[b], Hamed Pourkhorsandi[b], Geneviève Hublet[b], Philippe Claeys[a]

[a] *Analytical-, Environmental-, and Geo-Chemistry, Vrije Universiteit Brussel, Pleinlaan 2, BE-1050 Brussels, Belgium.*
[b] *Laboratoire G-Time, Université libre de Bruxelles, CP 160/02, 50, Av. F.D. Roosevelt, BE-1050, Brussels, Belgium.*
* Corresponding author. *E-mail address*: Ryoga.Maeda@vub.be (R. Maeda)

Abstract

Long-lived radioactive isotope systematics, such as Sm-Nd and Lu-Hf, are useful tools as important chronometers and tracers for chemical differentiation processes. Even though Antarctic meteorites include rare meteorites such as ungrouped, shergottites-nakhlites-chassignites, and lunar meteorites, the effects of Antarctic alteration on the Sm-Nd and Lu-Hf systems in chondrites have not yet been evaluated in detail. Moreover, the heterogeneity of Sm-Nd and Lu-Hf data in bulk chondrites prevents the determinations of precise average Sm-Nd and Lu-Hf values for individual chondrite groups and such robust values of the Chondritic Uniform Reservoir (CHUR). To examine the effects of Antarctic alteration and sample heterogeneity on the Sm-Nd and Lu-Hf isotope systematics, ten Antarctic H chondrites (HCs) and three HCs from hot deserts were characterized for their modal abundances, major and trace elemental concentrations, as well as Sm-Nd and Lu-Hf isotopic compositions. Regardless of the classical weathering index for Antarctic meteorites and the normalized Rb abundance used as a chemical alteration indicator in this study, the modal and elemental abundances in Antarctic HCs appear to be in good agreement with those in non-Antarctic HCs. The Sm-Nd and Lu-Hf isotopic compositions of the characterized H chondrites fall within the range measured for both HC falls and for falls of other chondrite classes, except in the case of the most heavily altered samples. Consequently, the effects of Antarctic alteration processes on the Sm-Nd and Lu-Hf systematics in HCs appear to be limited, except in the case of A 09516 (H6). The latter meteorite exhibits severe mineralogical and chemical alteration, with considerable losses of even the rare earth elements (REEs), which are considered relatively immobile. The ^{147}Sm/^{144}Nd, ^{143}Nd/^{144}Nd, ^{176}Lu/^{177}Hf, and ^{176}Hf/^{177}Hf of bulk HCs correlate with their P/Mg and Y/Mg. Furthermore, the Lu-Hf ratios are strongly correlated with their P/Ca and Y/Ca as well as their P/Mg and Y/Mg. Thus, the distribution of the elements between constituent minerals in ordinary chondrites (OCs) may control the heterogeneity observed for the bulk Sm-Nd and Lu-Hf data. In this context, the weight ratio of Ca-phosphates to Ca-pyroxene, or at least that of Ca-phosphates to silicates, may be a key factor leading to the observed elemental and isotopic variations. This observation indicates that the nugget effect of Ca-phosphates in OCs as the result of insufficient homogenization or terrestrial alteration leads to the heterogeneities displayed by the Sm-Nd and Lu-Hf data. Moreover, it also indicates that the use of equilibrated OCs for the determination of Sm-Nd and Lu-Hf data is affected more by sample heterogeneity, especially with respect to Ca-phosphates, than is the case for unequilibrated OCs, based on the re-distribution of REEs during thermal metamorphism on their parent bodies. This study demonstrates that Antarctic meteorites commonly preserve their original Sm-Nd and Lu-Hf isotopic compositions as much as chondrite falls, although exceptions are possible in the case of severe alteration. Similar to previous studies, we recommended the use of unequilibrated chondrites, for which the re-distribution of REEs is less extensive, for the determination of well-constrained average Sm-Nd and Lu-Hf isotopic compositions for individual chondrite groups as well as that of the robust Sm-Nd and Lu-Hf CHUR values.

1 INTRODUCTION

In 1969, a Japanese expedition found nine meteorites in Antarctica, which in 1973 led to the first systematic meteorite recovery expedition on the Southern continent (Yamaguchi *et al*., 2021), which was followed by expeditions until the present (*e.g.*, Goderis *et al*., 2021). Today, Antarctic meteorites constitute by number more than half of all known meteorites and include many rare varieties such as ungrouped chondrites and achondrites, shergottites-nakhlites-chassignites, and lunar meteorites (Meteorite Newsletter, NIPR; Antarctic Meteorite Newsletter, NASA). Hence, the Antarctic meteorite collection plays a pivotal role in understanding the history of the Solar System. Meteorites recovered after observed fall events are termed “falls”; those that cannot definitely be associated with observed falls, such as Antarctic meteorites, are named “finds.” Finds are generally characterized by a much longer terrestrial residence time than falls (roughly of the order of tens of kyr: *e.g.*, Al-Kathri *et al*., 2015). Many finds become weathered during this long residence time, and this process can take place relatively rapidly, particularly in temperate and tropical zones, as well as in hot deserts (Bland *et al*., 2006; Pourkhorsandi *et al*., 2021). On average, Antarctic meteorites exhibit old terrestrial ages, on the order of hundreds of kyr (*e.g.*, Nishiizumi *et al*., 1989), and these are better protected from terrestrial weathering while buried in the ice compared to finds collected from hot deserts (Whillans and Cassidy, 1983; Cassidy and Whillans, 1990). However, these meteorites were exposed to the extreme Antarctic climate during an extended period of time, leading to significant mineralogical and chemical alteration (*e.g.*, Koebel and Cassidy, 1991; Bland *et al*., 2006).

Rare earth elements (REEs) are refractory lithophile elements that share similar chemical properties due to their electron configurations, implying that they should not have been fractionated by condensation and volatilization processes in the early Solar System or by metal-silicate separation during core formation in differentiated planets. Therefore, REEs are universally used for understanding specific planetary processes, such as silicate differentiation. The REEs include long-lived radioactive isotopes such as ^{147}Sm and ^{176}Lu, which decay to ^{143}Nd (half-life ~106 Gyr; Lugmair and Marti, 1978) and ^{176}Hf (half-life ~37.1 Gyr; Patchett *et al*., 2004), respectively. Their isotope systematics form the basis of important chronometers and tracers of chemical differentiation processes. The Sm-Nd and Lu-Hf isotope systematics of chondritic meteorites are particularly important as the Chondritic Uniform Reservoir (CHUR), which constitutes the average reference for undifferentiated planetary material in the Solar System (DePaolo and Wasserburg, 1976). Bouvier *et al*. (2008) determined the currently most precise CHUR values of the Sm-Nd and Lu-Hf data as well as the respective isochrons by utilizing unequilibrated carbonaceous, ordinary, and enstatite chondrites of petrologic types 1-3, mostly from falls, since scatter increases when using equilibrated chondrites. Consequently, the Sm-Nd and Lu-Hf CHUR values are regarded as the equivalents of the composition of Bulk Silicate Earth. As Bouvier *et al*. (2008) discussed, the heterogeneity of Sm-Nd and Lu-Hf data in bulk chondrites is one of the largest problems when willing to determine precise average values (*i.e.*, CHUR values or an average of a group of chondrites), as the observed spread leads to larger uncertainties on the mean. For example, such heterogeneity occurs even on a duplicate analysis of Lu-Hf values in an H4 chondrite (^{176}Lu/^{177}Hf = 0.0301 ± 0.0002 and 0.0334 ± 0.0002, ^{176}Hf/^{177}Hf = 0.282444 ± 0.000009 and 0.282761 ± 0.000016 in Ochansk; Patchett *et al.*, 2004).

Previous studies regarding Sm-Nd and Lu-Hf systems in bulk chondrites have focused on falls to avoid any possible weathering occurring during long terrestrial residence (*e.g.*, Jacobsen and Wasserburg, 1984; Blichert-Toft and Albarède, 1997, Patchett *et al*., 2004; Bouvier *et al*., 2008). Terrestrial weathering can affect REEs, although they are often considered to be relatively immobile (*e.g.*, Shimizu *et al*., 1983; Crozaz, 2003; Al-Kathri *et al*., 2015; Pourkhorsandi *et al*., 2017). The effects of Antarctic alteration on REE abundances were only examined for achondrites, and more specifically for eucrites (Shimizu *et al*., 1983; Mittlefehldt and Lindstrom, 1991; Crozaz, 2003). Today, few studies exist for chondrites (Tatsumoto *et al*., 1981; Nishikawa *et al*., 1990). In particular, the effects of Antarctic alteration on the Sm-Nd and Lu-Hf systems in bulk chondrites remain poorly understood.

As such, even though the Antarctic collection includes meteorite groups and clans found only in Antarctica, the effects of Antarctic alteration on Sm-Nd and Lu-Hf systems in chondrites have not been assessed on a systematic way. Therefore, in this study, the results of the Sm-Nd and Lu-Hf isotope systematics in Antarctic HCs are examined in a methodical manner to evaluate weathering effects induced by extended residence times within the Antarctic ice. Moreover, this work also investigates the constituent minerals that control the heterogeneity of these isotope systems in bulk HC by combining the isotopic ratios and elemental abundance ratios, which can aid in determining average Sm-Nd and Lu-Hf isotopic compositions with limited uncertainty (*i.e.*, precise average Sm-Nd and Lu-Hf isotopic compositions) for individual chondrite groups.

2 EXPERIMENTAL

2.1 Samples

Ten Antarctic HCs and three HCs collected from hot deserts have been characterized for their modal abundances, and elemental and isotope compositions. Four of the Antarctic HCs, Asuka (A) 09436 (H3), A 09387 (H4), A 09618 (H5), A 09516 (H6), and the three hot desert HCs, northwest Africa (NWA) 6752 (H3), NWA 6771 (H4), and Sahara 97035 (H5), were provided by the Royal Belgian Institute of Natural Sciences (RBINS), Belgium. Meteorites A-881258 (H3.0), A-880941 (H3.3), Yamato (Y-)793574 (H3.5), Y-790461 (H3.7), Allan Hills (ALH) 78084 (H3.9), and Y-790960 (H7) were allocated by the National Institute of Polar Research (NIPR), Japan. Available information on the meteorites is listed in Table 1. To clarify any potential effect of terrestrial weathering on the inner portions of these chondrites - even if the sample visually appears fresh -, only the interior portions were used to avoid as much as possible fusion crust or sample fragments directly affected by terrestrial weathering.

2.2 *In-situ* measurement

Polished thick sections were prepared for all of the meteorites, except in the case of NWA 6752 (H3) when a polished thin section was used. These polished thick and thin sections were analyzed using a Bruker M4 Tornado micro-X-ray fluorescence (μXRF) scanner equipped with a Rh source and two XFlash 430 Silicon Drift detectors at the Vrije Universiteit Brussel (VUB), Belgium. The M4 set up is described in detail in Winter and Claeys (2017), and for each sample, elemental maps of 16 elements (Na, Mg, Al, Si, P, S, Cl, K, Ca, Ti, Cr, Mn, Fe, Ni, and Zn) were obtained. To produce the element maps, the 25 μm X-ray beam was applied under vacuum conditions (20 mbar), with 10 μm step size, 1 ms dwell time per point and maximized source energy settings (50 kV, 600 μA) without a source filter. Constituent minerals in the samples were identified from the elemental maps and their modal abundances were determined using the ImageJ image analysis program, while confirming the nature of these phases using a JEOL JSM-IT300 scanning electron microscope (SEM) equipped with an Oxford energy dispersive spectrometer (EDS) at the SURF research unit of VUB. Uncertainties for the modal abundances determined using this method are estimated to be better than 10% relative.

2.3 Bulk analyses

To examine the effects of sample heterogeneity as well as Antarctic weathering on the Sm-Nd and Lu-Hf systems, a relatively small sample volume was preferred in this study to amplify sample heterogeneity caused by sampling. Approximately 200 mg of fragments of each sample were homogenized using an agate mortar and pestle dedicated to chondrites. No leaching to remove terrestrial materials was applied, even in the case of the three hot desert HCs. Approximately 100 mg of each powdered sample, which is the smallest possible amount to measure the elemental abundances and the isotope compositions based on their detection limits, was dissolved in Teflon beakers using a mixture of ultrapure concentrated HF-HNO_3 (1:3) at 120 °C overnight. Because undigested residue remained in the beakers, possibly including acid-resistant phases such as oxides, the residues were then transferred into Teflon bombs for high-pressure dissolution, using the same acid mixture at 150 °C for 2 days. During the high-pressure dissolution, the supernatants remaining in the first Teflon beaker were evaporated. After the high-pressure dissolution, the solutions in the bombs were added to the Teflon beakers containing the residues of the supernatants. Following evaporation, the residues were dissolved in concentrated HCl and evaporated again. After re-dissolution in 1.5 M HCl with a trace amount of concentrated HF, a ~2% aliquot of each solution was taken for the determination of major and trace elemental abundances. Similarly, a ~5% aliquot of each solution was spiked with mixed ^{148}Nd-^{150}Sm and ^{176}Lu-^{179}Hf spikes. The spiked aliquots were heated on a hotplate for at least 1 day for spike-sample equilibration.

The REEs and Hf were separated from the main fraction by cation exchange chromatography using 2 mL of AG50W-X8 resin (100-200 mesh for the spiked aliquots, 200-400 mesh for the unspiked aliquots). The Hf cut was collected first during the loading of the sample and the following rinsing step using 1.5 M HCl with a trace amount of concentrated HF, while the REE cut was subsequently collected using 6 M HCl. The

REE cuts were loaded onto a column with 2 mL of HDEHP resin to separate Nd for both the unspiked and spiked aliquots, and Sm and Lu for the spiked aliquots. The Hf cuts were further purified from Fe by anion exchange chromatography in 6 M HCl using 2 mL of AG1X8 resin (100-200 mesh for the spiked aliquots, 200-400 mesh for the unspiked aliquots), and the remaining matrix, especially Ti, was removed on 2 mL of Eichrom LN-Spec resin using 6 M HCl with a trace amount of H_2O_2. Finally, Hf was collected in 4 M HF. The yields of Nd, Sm, Lu, and Hf are estimated to be better than 90%, 95%, 95%, and 90% respectively, for both unspiked and spiked aliquots (Debaille *et al.*, 2007). Total procedural blanks were determined to be ≤ 26 pg and ≤ 10 pg for Nd and Sm, respectively, and ≤ 4.5 pg and ≤ 20 pg for Lu and Hf, respectively. No blank correction was applied due to these negligible blank levels, even on the spiked aliquots (the blank-to-sample rations of more than 1%) because they represent insignificant contributions. The chemical procedures outlined here were performed at the Université libre de Bruxelles (ULB), Belgium, and are based on procedures described in detail in Armytage *et al.* (2018) and Debaille *et al.* (2007, 2017). Reference basalt BHVO-2 of the United States Geological Survey was subjected to the same procedures and measured in duplicate to validate the analytical accuracy and reproducibility during the following measurements using inductively coupled plasma-optical emission spectrometry (ICP-OES), quadrupole-ICP-mass spectrometry (Q-ICP-MS), and multiple collector-ICP-MS (MC-ICP-MS). Approximately 50 mg of BHVO-2 was weighed and prepared at similar concentrations for measurement to the chondrite samples for both unspiked and spiked aliquots. Samples A 09436 (H3) and A 09516 (H6) were also analyzed in duplicate. All duplicate analyses were carried out on different powder subsamples.

2.3.1 Measurement of major and trace elemental abundances using ICP-OES and Q-ICP-MS

The major elemental abundances (Na, Mg, Al, P, K, Ca, Ti, Cr, Mn, Fe, Co, and Ni) were determined using a Thermo Scientific iCAP 7000 Plus Series ICP-OES at ULB. Yttrium was used as the internal standard, and the dilution factors (DFs) for the meteorite samples and the reference basalt were set to be 15,000 and 10,000 respectively, using 5% HNO_3.

The trace elemental abundances (Cu, Zn, Rb, Sr, Y, Zr, Nb, Ba, REEs, Hf, Th, and U) were determined using an Agilent 7700 ICP-MS at ULB. Measurement solutions were prepared with 5% HNO_3 and all of the measured elements including the high field strength elements were analyzed in 5% HNO_3 without HF. For Q-ICP-MS analysis, In was used as the internal standard, and the DFs for the meteorite samples and the geological reference materials were set to be 2,000 and 6,000, respectively, in order to minimize the influence of non-spectral matrix effects (Ebihara *et al.*, 2020). Although slight analyte loss has been observed during dissolution (Ebihara *et al.*, 2020), no correction for such analyte loss was applied here. Individual single element standards of Ba, Ce, Pr, and Nd were used to correct isobaric interferences from their oxide molecules. The results for the elemental abundances of BHVO-2 (n = 2) are shown in Table 2, together with their preferred values (Jochum *et al.*, 2016).

2.3.2 Isotope ratio measurement using MC-ICP-MS

All of the unspiked and spiked cuts were analyzed in 0.05 M HNO_3 (with 0.05 M HF for the Hf cuts) using the Nu instruments MC-ICP-MS Nu-Plasma II equipped with an Aridus II desolvating nebulizer at

ULB. For isotope measurements of Nd, the unspiked Nd cuts were diluted to 20 ppb. The isobaric interference of ^{144}Sm on ^{144}Nd was monitored on mass ^{147}Sm, but no Sm was detected. Measured Nd isotope ratios were normalized to ^{146}Nd/^{144}Nd = 0.7219 using an exponential law following Debaille *et al.* (2007) to correct for instrumental mass fractionation. Measurements of the meteorite samples and BHVO-2 were bracketed by the measurement of a 20 ppb Rennes in-house Nd standard. The measured ^{143}Nd/^{144}Nd values of the standard were re-calculated to the accepted ^{143}Nd/^{144}Nd value of the Rennes in-house Nd standard (0.511961; Chauvel and Blichert-Toft, 2001). For isotope measurements of Hf, the unspiked Hf cuts were prepared at 5 ppb. Isobaric interferences for Hf from Yb, Lu, and W were monitored on masses ^{172}Yb, ^{175}Lu, and ^{182}W, respectively. No detectable Yb, Lu, or W were found in the unspiked Hf cuts. Measured Hf isotope ratios were normalized to ^{179}Hf/^{177}Hf = 0.7325 using the exponential law to correct for instrumental mass fractionation. A 5 ppb JMC-475 Hf standard was used to bracket each sample during the runs. The measured ^{176}Hf/^{177}Hf values of the Hf standard were re-calculated to the accepted ^{176}Hf/^{177}Hf value of the JMC-475 Hf standard (0.282163; Blichert-Toft *et al.*, 1997). Internal reproducibilities of Nd and Hf are better than 32 ppm and 31 ppm for all standards, respectively. The means of ^{143}Nd/^{144}Nd values and ^{176}Hf/^{177}Hf values in BHVO-2 are 0.512971 ± 0.000012 (2SE, n = 4) and 0.283102 ± 0.000011 (2SE, n = 10), as shown in Table 2. These values overlap within uncertainty with published reference values (0.512984 ± 0.000011; Weis *et al*, 2006 and 0.283105 ± 0.000011; Weis *et al*, 2007, respectively).

For spiked cuts, the mass fractionation for each element was corrected using an exponential law followed by spike stripping using an iterative method (Debaille *et al.*, 2007). The same isotopes as in unspiked Nd and Hf analyses were monitored to check for isobaric interferences during spiked Nd and Hf analyses. No detectable contributions of these isotopes were observed in the spiked Nd and Hf cuts. During Sm measurement, ^{147}Sm, ^{150}Sm, ^{152}Sm, and ^{154}Sm were measured. Here, ^{150}Sm is included due to the use of the ^{150}Sm enriched spike despite the isobaric interference by ^{150}Nd. The presence of Nd and Gd in the Sm cuts was monitored on masses ^{146}Nd and ^{156}Gd, and the presence of Gd was corrected mathematically. Even though a trace of Nd was observed in the Sm cuts, the contribution was considered negligible. The isobaric interference of ^{176}Hf was monitored on mass ^{177}Hf during Lu analysis, but no Hf was detected in the Lu cuts. Because Lu possesses only two stable isotopes, a mass fractionation correction for Lu must be applied, for example by using Yb (Blichert-Toft *et al.*, 1997). The uncertainties on the Nd, Sm, Lu, and Hf concentrations are dominated by the uncertainty of the spike calibration, which is estimated to be better than 0.5% (2SE). Therefore, the uncertainties on the concentrations are estimated to be 0.5% as a maximum and are presented in Tables 2 and 4. The obtained ^{147}Sm/^{144}Nd and ^{176}Lu/^{177}Hf values for BHVO-2 are 0.1515 ± 0.0011 (2SE) and 0.0088 ± 0.0001 (2SE), shown in Table 2, which are in good agreement with their preferred values of 0.1501 ± 0.0010 and 0.00878 ± 0.00006, respectively (Jochum *et al.*, 2016).

3 RESULTS

3.1 Modal abundances

Table 3 summarizes the modal abundances in all samples obtained using the µXRF, including the mean values of unequilibrated H chondrites (UHCs; n = 7) and equilibrated H chondrites (EHCs; n = 6), together with the published modal abundances of EHCs (Van Schmus, 1969; McSween *et al.*, 1991). According to the mineral observation using SEM-EDS in this study, forsterite, silica, and a few accessory minerals (Table 3) can be found in a limited number of samples. Also, H chondrites generally contain ilmenite (~0.2 wt.%: *e.g.*, McSween *et al.*, 1991). However, the mapping using µXRF is not sufficiently quantitative and the minimum spot size (25 µm) used in this study is larger than the size of some mineral phases (*e.g.*, silica and ilmenite), which does not allow distinguishing forsterite from low-Ca pyroxene (especially enstatite), silica from feldspar, or ilmenite from chromite. Therefore, the modal abundances of low-Ca pyroxene, feldspar, and chromite obtained in this study include the abundances of forsterite, silica, and ilmenite, respectively. Moreover, grains smaller than ~5 µm, such as tiny Ca-phosphates especially present in UHCs, might have been missed because of this limitation. However, forsterite and silica are only observed in some UHCs (for forsterite: A-881258, Y-793574, Y-790461, and NWA 6752; for silica: Y-790461 and A 09436) and A 09387 (H4), and these were confirmed to be present in the HCs in trace abundances only. Based on this work, there is no resolvable difference in the modal abundances between Antarctic HCs and hot desert HCs, thus the mean values of UHCs and EHCs are calculated from the combined data for Antarctic and hot desert HCs (Fig. 1). Most of the mean modal abundances in UHCs and EHCs are in good agreement with each other (Table 3 and Fig. 1). These mean modal abundances also compare well with the published values listed in Table 3. The mean modal abundance of total Ca-phosphates in EHCs is 0.70 ± 0.10 wt. % at the 95% confidence interval (95% CI) and agrees within uncertainty with previously published values. In addition, the mean modal abundances of chlorapatite and merrillite in UHCs and EHCs overlap within uncertainty (0.10 ± 0.07 wt. % vs. 0.17 ± 0.14 wt. % and 0.29 ± 0.08 wt. % vs. 0.53 ± 0.24 wt. %, respectively at the 95% CI; Table 3). However, the mean modal abundance of total Ca-phosphates in UHCs is 0.39 ± 0.09 wt. % (95% CI), which is significantly lower than the abundance in EHCs (Fig. 1).

3.2 Elemental abundances

The major and trace elemental abundances in bulk samples measured using ICP-OES and ICP-MS are summarized in Table 4, with mean values for the Antarctic UHCs (n = 7), Antarctic EHCs (n = 3), Antarctic HCs (n = 10) and hot desert HCs (n = 3), and literature values for non-Antarctic HCs (Jarosewich, 1990 for Na. Mg, Al, P, K, Ca, Ti, Cr, Mn, Fe, and Ni; Wasson and Kallmeyn, 1988 for Cu, Zn, Rb, Sr, Y, Zr, Nb, Ba, and Hf; Nakamura, 1974 for REEs; Tatsumoto *et al*, 1973 for Th and U). The data of A 09516 (H6) are excluded from the mean values of Antarctic EHCs and Antarctic HCs because of the anomalous depletions in various elements, including the REEs, displayed by this sample as the result of chemical alteration in Antarctica (*e.g.*, Lipschutz and Samuels, 1991). This sample also exhibits a positive Eu anomaly, as often observed in heavily weathered Antarctic chondrites (*e.g.*, Y-74014: Ebihara, 1986; Y-74492: Nishikawa *et al.*, 1990). The characteristics of this sample are described in detail in subsection 4.1.2.

3.2.1 Major elements

The abundances of major elements for individual samples obtained using ICP-OES were determined with ~2% relative standard deviation (RSD; 1SD) on average, while the individual RSDs ranged from 0.05% to 8%. Although most of the mean values for major elemental abundances in Antarctic HCs are in good agreement with the literature values, the mean values of K, Ti, Fe, and Ni are ~15% lower than those reported in literature. However, the mean Ti abundance in Antarctic HCs is in excellent agreement with the published Ti abundance in HCs determined using the isotope dilution method (0.0549 ± 0.0015 wt. % at the 95% CI; calculated from Shima, 1979). According to these results, there is almost no difference in the abundances of major elements between Antarctic and hot desert HCs, although the K and Ca abundances in hot desert HCs are ~20% higher than those in Antarctic HCs possibly due to either mobilization of these elements by chemical alteration in Antarctica (Velbel *et al*. 1991) or terrestrial contamination in hot deserts (Al-Kathiri *et al*., 2005; Pourkhorsandi *et al*., 2019).

3.2.2 Trace elements

The trace elemental abundances for individual samples obtained using Q-ICP-MS are reproducible within ~3% RSD (1SD) on average. The abundances of Lu and U in some samples display larger uncertainties, due to their lower absolute abundances, on the order of ~10% RSD. The CI-normalized REE, Th, and U abundances in each sample are shown in Fig. 2, and their mean REE, Th and U abundances in Antarctic UHCs, EHCs, and HCs are compared with the literature values in Fig. 3 (CI values are from Anders and Grevesse, 1989). No resolvable difference is observed between the trace elemental abundances of bulk Antarctic UHCs and EHCs, which is consistent with the conclusions of Huss *et al*. (2006) and Hublet *et al*. (2019). Most of the mean trace elemental abundances in Antarctic HCs, especially for REEs, Th, and U, are in good agreement with the literature values for non-Antarctic HC listed in Table 4. The mean values for Sr and Ba in Antarctic HCs deviate from the literature values (8.82 ± 0.31 ppm vs. 10 ppm and 3.22 ± 0.15 ppm vs. 4.20 ppm at the 95% CI, respectively). However, Sr and Ba are strongly affected by terrestrial weathering as their abundances in the hot desert HCs characterized in this study are high (16.9-70.9 ppm and 17.8-166 ppm, respectively). Moreover, the mean values for Sr and Ba in Antarctic HCs are in agreement within uncertainty with their published values for Antarctic HCs determined by the isotope dilution method (9.29 ± 0.93 ppm and 2.69 ± 0.75 ppm at the 95% CI; Nishikawa *et al*., 1990). Thus, the observed deviations may only reflect a difference between Antarctic and non-Antarctic meteorites. For hot desert HCs, the mean values of Cu, Zn, Rb, and Y agree within uncertainty with those for Antarctic HCs in this study and with the literature values for non-Antarctic HC, with the exception of Rb. However, other trace elements are enriched compared with the values of Antarctic HCs and non-Antarctic HCs, especially in the case of Sr, Ba, the light REEs (LREEs), Th, and U. In addition, negative Eu anomalies are observed in the CI-normalized REE patterns of hot desert HCs (Fig. 2).

3.3 Isotope compositions

The Nd, Sm, Lu, and Hf abundances determined by the isotope dilution method, and Sm-Nd and Lu-Hf isotopic compositions in the bulk samples measured using MC-ICP-MS are summarized in Table 2 (for BHVO-2) and Table 4 (for meteorites) as well as in Figs. 4 and 5. The ^{143}Nd/^{144}Nd and ^{176}Hf/^{177}Hf values in most of the samples were determined within 20 ppm relative standard error (RSE) and 60 ppm RSE (2SE), respectively. This relatively large standard error for ^{176}Hf/^{177}Hf values compared with that for ^{143}Nd/^{144}Nd values clearly results from the difference in the adjusted concentrations in the measurement solutions (see subsection 2.3.2). Furthermore, the actual Hf concentration in the measurement solutions for most of the meteorite samples was less than 5 ppb, leading to larger standard errors for the ^{176}Hf/^{177}Hf values. On the other hand, the differences in these elemental abundances between those determined using the isotope dilution method (MC-ICP-MS) and calibration line method (Q-ICP-MS) are less than 5% on average, which is in excellent agreement.

The mean values of the elemental abundances determined using the isotope dilution method in Antarctic HCs are in excellent agreement with those in HC falls (Table 4). Most of the Sm-Nd and Lu-Hf data for Antarctic HCs are within the range of chondrite fall data and several of them plot on the respective chondrite isochrons within uncertainty (for Sm-Nd data: Jacobsen and Wasserburg, 1980, 1984; Patchett *et al*., 2004; Boyet and Carlson, 2005; Carlson *et al*., 2007; Bouvier *et al*., 2008, Gannoun *et al*., 2011; Burkhardt *et al*., 2016; Fukai and Yokoyama, 2017; for Lu-Hf data: Blichert-Toft and Albarède, 1997; Bizzarro *et al*., 2003; Patchett *et al*., 2004; Bouvier *et al*., 2008; Dauphas and Pourmand, 2011; for chondrite isochrons: Bouvier *et al*., 2008). The mean values of ^{147}Sm/^{144}Nd, ^{143}Nd/^{144}Nd, ^{176}Lu/^{177}Hf, and ^{176}Hf/^{177}Hf for Antarctic HCs overlap with those of HC falls within uncertainties (Table 4). There are no resolvable differences in the mean values of Antarctic UHC and EHC. In the case of hot desert HCs, the ^{147}Sm/^{144}Nd and ^{143}Nd/^{144}Nd values (0.1578-0.1866 and 0.512312-0.512540, respectively) are significantly lower than the mean values reported in literature for HC falls (0.1953 ± 0.0006 and 0.512623 ± 0.000009 at 2SE, respectively; Table 4) and the mean values determined here for Antarctic HCs (0.1971 ± 0.0016 and 0.512633 ± 0.000044 at the 95% CI, respectively; Table 4), plotting as far from the isochron as falling out of the range of chondrite fall data (Fig. 4). In contrast, it seems that the ^{176}Lu/^{177}Hf and ^{176}Hf/^{177}Hf values of hot desert HCs fall within the ranges determined in literature and measured for Antarctic HCs (Table 4 and Fig. 5), except in the case of NWA 6771 (H4), which is characterized by an anomalously high Hf abundance (269 ppb).

4 DISCUSSION

4.1 Assessment of weathering effects on the Sm-Nd and Lu-Hf systems in Antarctic HCs

For the assessment of weathering effects on Antarctic meteorites, the classical ABC index system is commonly used: A—minor rustiness (*e.g.*, rust stains along fractures are minor); B—moderate rustiness (*e.g.*, 7.5 to 35% of metal particles are weathered to limonite); C—severe rustiness (*e.g.*, most metal particles are weathered to limonite); and e—evaporite minerals are visible to the naked eye (Antarctic Meteorite Newsletter, NASA; Meteorite Newsletter, NIPR). However, this index may not be sufficient as an indicator especially in terms of chemical alteration (Koebel and Cassidy, 1991), as it is determined based on mineralogy. Velbel (1988) and Nishikawa *et al*. (1990) found that bulk Rb abundances in some Antarctic ordinary chondrites (OCs) and heavily weathered non-Antarctic HCs are anomalously low and do not co-vary with the weathering index. Velbel (1988) concluded that Rb loss could be due to chemical leaching during the residence of the meteorite in Antarctica, indicating that relative loss of Rb may be a better indicator of chemical alteration than the weathering index. The results presented here display remarkable deviations in the Rb abundances of both Antarctic and hot desert HCs relative to those reported in literature (Table 4). The mean Rb abundance of Antarctic HCs is significantly lower than the literature value (2.26 ± 0.34 ppm vs. 2.9

ppm at the 95% CI) with extremely low Rb abundances in A-880941 (H3.3) and A 09516 (H6), implying a loss of Rb during Antarctic alteration. However, these lower Rb abundances may just reflect heterogeneity in the amount of feldspar in the samples, which may be induced as the result of a sampling bias (*i.e.*, sampling heterogeneity), as Rb is mostly distributed in feldspar (Shima and Honda, 1968; Mason and Graham, 1970). The average Na and Al abundances in the bulk samples are used as an indicator for the amount of feldspar in the sample, and the respective Rb abundances normalized to the indicator are listed in Table 5. Even considering the heterogeneous distribution of feldspar based on these normalized Rb abundances, the samples displaying extremely low Rb abundances also show low normalized Rb abundances. Thus, any possible effect on the bulk Rb abundance by sampling biases alone can be ruled out. The normalized Rb abundances can also be compared with the normalized abundances of Sr, which is especially concentrated in feldspar (Shima and Honda, 1968; Mason and Graham, 1970) but generally considered less mobile than Rb. The data from this study are compared with calculated values for non-Antarctic HC (Table 4) and Antarctic HCs from Nishikawa *et al.* (1990), in Fig. 6. The normalized Sr abundances in most of the samples are in good agreement with the literature values, but in various samples the normalized Rb abundances are lower than those reported in literature and display a wider range than the Sr abundances. A similar trend emerges when comparing the normalized abundance of Rb and that of Ba, which is concentrated in feldspar as well (Table 5). The low normalized Rb abundances (< 2.7) in some Antarctic HCs co-vary to some degree with their weathering grades, although exceptions exist. A-880941 (H3.3) is categorized as A/B but contains a low normalized Rb abundance (1.77 ± 0.09), which may reflect a difference in the weathering degree implied by elemental ratios versus that inferred based on petrographic observation. In any case, the low Rb abundances clearly reflect the loss of Rb during the terrestrial residence of the meteorites in Antarctica or elsewhere in the world (Nishikawa *et al.*, 1990), possibly because of chemical leaching. Therefore, the normalized Rb abundances are taken here as a potential indicator for chemical alteration in the following discussions.

4.1.1 Weathering effects on bulk Sm-Nd and Lu-Hf systems

The Sm-Nd and Lu-Hf data of a few Antarctic HCs (*e.g.*, A 09516) plot away from the respective chondrite isochrons (Figs. 4 and 5). This may reflect an effect of weathering on the Sm-Nd and Lu-Hf systems in bulk chondrites in Antarctica. However, it remains unclear whether the parent isotopic ratios ^{147}Sm/^{144}Nd and ^{176}Lu/^{177}Hf or the daughter isotopic ratios ^{143}Nd/^{144}Nd and ^{176}Hf/^{177}Hf have been affected by Antarctic weathering. Alternatively, it is also possible that both ratios were disturbed. Therefore, we need to consider one by one which of the following processes affected the Sm-Nd and Lu-Hf systems: i) sample heterogeneity, ii) thermal metamorphism on the parent body(ies), iii) contamination with terrestrial material, and iv) chemical alteration during residence on the Earth.

i) Based on the results of this study and previous works, REEs in bulk chondrites are largely unfractionated (*e.g.*, Huss *et al.*, 2006). On the other hand, REEs in individual constituent minerals are highly fractionated depending on their partition coefficients (*e.g.*, Curtis and Schmitt, 1979). This fractionation of REEs between the constituent minerals affects not only their abundances but also their radiogenic isotope systems (*e.g.*, Jacobsen and Wasserburg, 1983). Thus, a loss of constituent mineral(s) due to terrestrial weathering, as observed in Antarctic eucrites (Mittlefehldt and Lindstrom, 1991), or a non-representative sampling bias may induce minor variation in the elemental compositions and radiogenic isotope data of bulk chondrites. According to Amelin and Rotenberg (2004), Amelin (2005), and Debaille *et al*. (2017), the Sm-Nd and Lu-Hf data in individual minerals are indeed different from those in bulk chondrites. However, both data of individual minerals and bulk chondrites plot on the same chondrite isochron when considering the uncertainties. Therefore, the heterogeneous distribution of constituent mineral(s) due to a sampling bias or terrestrial weathering, *i.e.*, sample heterogeneity may result in heterogeneity of the Sm-Nd and Lu-Hf data of bulk chondrites, but the isotopic data will always plot along the isochrons.

ii) Thermal metamorphism can affect the Sm-Nd and Lu-Hf systems at the bulk scale as a redistribution due to crystallization of REE-rich minerals such as Ca-phosphates, can take place during metamorphism (Bouvier *et al*., 2008; Martin *et al*., 2013; Debaille *et al*., 2017; Bloch *et al*., 2017, 2018). The nugget effect, in which the REE-rich Ca-phosphates are heterogeneously distributed, can lead to sampling biases due to non-representative sample volumes, while such Ca-phosphate phases may also be preferentially weathered during the terrestrial residence of the meteorite of interest. These processes may produce wider ranges in the Sm-Nd and Lu-Hf data in bulk equilibrated chondrites than in bulk unequilibrated chondrites (Bouvier *et al*., 2008; Dauphas and Pourmand, 2011, 2015). However, as mentioned above, unequilibrated and equilibrated chondrites do not show any fractionation or change in the bulk REE abundances in most of the cases. If unequilibrated and equilibrated chondrites had originally the exact same bulk elemental composition, the bulk Sm-Nd and Lu-Hf data in these chondrites should exhibit the same values. This is consistent with the observation that the mean Sm-Nd and Lu-Hf values in bulk unequilibrated and equilibrated chondrites are in agreement with each other, both based on this study and literature values (Jacobsen and Wasserburg, 1980, 1984; Blichert-Toft and Albarède, 1997; Bizzarro *et al*., 2003; Patchett *et al*., 2004; Boyet and Carlson, 2005; Carlson *et al*., 2007; Bouvier *et al*., 2008, Dauphas and Pourmand, 2011; Gannoun *et al*., 2011; Burkhardt *et al*., 2016; Fukai and Yokoyama, 2017). Therefore, thermal metamorphism emphasizes the heterogeneity of the Sm-Nd and Lu-Hf data in bulk chondrites at the scale of the individual sample. Theoretically, the isotopic data in bulk unequilibrated and equilibrated chondrites should have the same values as long as these have the same elemental compositions.

iii) Considering the higher Nd, Sm, Lu, and Hf abundances and lower ^{147}Sm/^{144}Nd and ^{176}Lu/^{177}Hf in the upper continental crust (26 ppm, 4.5 ppm, 0.32 ppm, 5.8 ppm, 0.10, and 0.0079, respectively; Taylor and McLennan, 1995) as potential contaminating material relative to the lower REE concentrations in chondrites, the Sm-Nd and Lu-Hf data in bulk chondrites display lower values in most of the cases when terrestrial contamination occurred (Bast *et al*., 2017a, b; Pourkhorsandi *et al*., 2017, 2021). As the hot desert HCs used in this study exhibit enrichments in Sr, Ba, LREEs, Th, and U and negative Eu anomalies (Table 4 and Fig. 2), these enrichments must result from terrestrial contamination (*e.g.*, Al-Kathiri *et al*., 2005; Pourkhorsandi *et al*., 2017). Thus, the low ^{147}Sm/^{144}Nd and ^{143}Nd/^{144}Nd values in the hot desert HCs (Table 4 and Fig. 4) must also be explained by mixing with terrestrial material. However, the absolute Lu abundance in the upper continental crust is only ~10 times higher than that in HCs and Hf is highly immobile during terrestrial alteration, while the absolute abundances of Nd and Sm in the upper continental crust are ~45 and ~25 times higher than those in HCs, respectively (Taylor and McLennan, 1995), and these elements are also considered to be more mobile than Hf (Middelburg *et al*., 1988). In this way, because it is more difficult for the Lu-Hf system to be affected by terrestrial contamination than the Sm-Nd system, the ^{176}Lu/^{177}Hf and ^{176}Hf/^{177}Hf values in the hot desert HCs used in this study do not deviate as far from the isochron as observed for the ^{147}Sm/^{144}Nd, ^{143}Nd/^{144}Nd values (Table 4 and Fig. 5). This is consistent with the observation of Al-Kathiri *et al.* (2005) who showed that Hf abundances in HCs collected from hot deserts do not deviate from the literature value listed in Table 4 (0.15-0.18 ppm vs. 0.18 ppm), while their corresponding Nd and Sm abundances are ~10-30% higher than the literature values (0.66-0.75 ppm vs. 0.59 ppm and 0.21-0.24 ppm vs. 0.19 ppm, respectively). Therefore, although the extent of terrestrial contamination on chondrites strongly depends on where the sample was collected (Pourkhorsandi *et al.*, 2017, 2021), this process can produce deviations from the Sm-Nd and Lu-Hf isochrons in the case of chondrites (Bast *et al.*, 2017b). These deviations should be accompanied by additional indications of terrestrial contamination, such as higher abundances of Sr, Ba, LREEs, Th, and U.

iv) Chemical alteration during terrestrial residence, such as leaching, occurs anywhere on Earth in the presence of water, either in the form of rain or humidity. Even in Antarctica, melting of ice can trigger sample alteration (Mittlefehldt and Lindstrom, 1991). Chemical alteration is commonly divided into two main types: the first type encompasses alteration affecting minerals, such as the loss of Ca-phosphates (Mittlefehldt and Lindstrom, 1991), while the second type reflects alteration that depends on the mobility of the element, as in the case of Rb loss (Velbel, 1988; Nishikawa *et al.*, 1990). For the former type of alteration, the effect on the Sm-Nd and Lu-Hf systems is similar to the effect of sample heterogeneity. Thus, even if this alteration occurs, the affected Sm-Nd and Lu-Hf data would plot on their respective isochrons assuming no prior disturbance. The latter type of alteration can disturb these systems because the parent nuclide and the daughter nuclide may have different chemical characteristics, which is consistent with the observations of Nishikawa *et al.* (1990) although based on the Rb-Sr system. Thus, if this alteration occurred during the residence of the meteorite at the Earth's surface, the ^{147}Sm/^{144}Nd and ^{176}Lu/^{177}Hf values would be disturbed producing deviations from the Sm-Nd and Lu-Hf isochrons. This type of alteration does not influence the ^{143}Nd/^{144}Nd and ^{176}Hf/^{177}Hf values at the bulk scale.

In summary, thermal metamorphism amplifies the nugget effect of REE-rich minerals such as Ca-phosphates on the Sm-Nd and Lu-Hf isotope systems. Sample heterogeneity also affects the Sm-Nd and Lu-Hf data in bulk chondrites, but the measured data continue to plot on the respective chondrite isochrons. In addition, ^{143}Nd/^{144}Nd and ^{176}Hf/^{177}Hf values are not affected by chemical alteration at the bulk scale or at least such isotopic fractionation is not yet resolvable. Thus, the ^{143}Nd/^{144}Nd and ^{176}Hf/^{177}Hf values obtained likely reflect the original values of the bulk HC sample, unless this sample was contaminated by terrestrial material. Because the Asuka, Yamato, and Allan Hill samples used in this study are collected from blue ice fields, it is unlikely that the samples were contaminated during their residence in Antarctica. Therefore, the deviations from the isochrons on the Sm-Nd and Lu-Hf data that are apparent in a small set of samples (Figs. 4 and 5) have likely been produced by disturbance of the ^{147}Sm/^{144}Nd and ^{176}Lu/^{177}Hf values during the chemical alteration that depends on the elemental mobility.

Based on the assumption above, to evaluate the effects of Antarctic weathering on the Sm-Nd and Lu-Hf data in bulk chondrites, the differences in ^{147}Sm/^{144}Nd and ^{176}Lu/^{177}Hf values between the measured values and the respective chondrite isochrons are expressed as δ^{147}Sm/^{144}Nd (‰) and δ^{176}Lu/^{177}Hf (‰) respectively, calculated following the equations (in the case of the Sm-Nd system):

$$\delta\frac{^{147}Sm}{^{144}Nd} = \left[\left(\frac{^{147}Sm}{^{144}Nd}\right)_{measured} - \left(\frac{^{147}Sm}{^{144}Nd}\right)_{ideal}\right] \times 1{,}000\ [‰]$$

and

$$\left(\frac{^{147}Sm}{^{144}Nd}\right)_{ideal} = \frac{\left(\frac{^{143}Nd}{^{144}Nd}\right)_{measured} - b}{a}$$

where *a* is the slope of the isochron and *b* is the intercept of the isochron, which is the initial ^{143}Nd/^{144}Nd value. The values for the isochrons and the initial isotope ratios in Sm-Nd and Lu-Hf systems are from Bouvier *et al.* (2008). These calculated differences for Antarctic HCs reflect the extent of the disturbance on the ^{147}Sm/^{144}Nd and ^{176}Lu/^{177}Hf values by Antarctic alteration. The calculated differences are shown in Fig. 7, with a range of differences in chondrite falls since the Sm-Nd and Lu-Hf data in chondrite falls also show a deviation from the isochron (Figs. 4 and 5). According to Fig. 7, the δ^{147}Sm/^{144}Nd values of Antarctic HCs, except for A 09436 (H3)-2, ALH 78084 (H3.9), and A 09516 (H6), fall within the range of HC falls taking into account the associated uncertainty. The δ^{176}Lu/^{177}Hf of Antarctic HCs, except for Y-793574 (H3.5), Y-790461 (H3.7), A 09387 (H4), and A 09618 (H5), also fall within the range of HC falls. Although the δ^{147}Sm/^{144}Nd or δ^{176}Lu/^{177}Hf values of the samples excluded above do not fall within the range of HC falls, the δ^{147}Sm/^{144}Nd and δ^{176}Lu/^{177}Hf values of all Antarctic HCs, except for A 09516 (H6)-1, do plot within the range of other chondrite falls. The values of Antarctic HCs that do not fall within the range of HC falls could indicate disturbance of the systems by chemical alteration in Antarctica. However, this disturbance can be considered minor as most of the values fall within the range of other chondrite falls. The δ^{147}Sm/^{144}Nd and δ^{176}Lu/^{177}Hf values in A-880941 (H3.3), which displays the lowest weathering index but the second highest Rb loss in this study, fall close to 0. Similar δ^{147}Sm/^{144}Nd and δ^{176}Lu/^{177}Hf values are observed for heavily weathered (sub)samples A 09618 (H5) and A 09436 (H3)-2 respectively, and for A-881258 (H3.0) that indicates no Rb loss. Furthermore, δ^{147}Sm/^{144}Nd and δ^{176}Lu/^{177}Hf values of all published data for Antarctic chondrites (Figs. 4 and 5), except for ALHA 77295 (EH3) with a high δ^{147}Sm/^{144}Nd (5.66‰), range from -1.96 to 1.94‰ and from -0.02 to 0.18‰, respectively, falling within the range of chondrite falls also regardless of their weathering index. Therefore, it can be concluded that Antarctic chondrites display limited effects of weathering on their isotopic values, and the extent of the disturbance on ^{147}Sm/^{144}Nd and ^{176}Lu/^{177}Hf in Antarctic chondrites would be of a level similar to that measured for chondrite falls even if Antarctic weathering occurred. In addition, there seems to be no correlation between the δ^{147}Sm/^{144}Nd and δ^{176}Lu/^{177}Hf values and the weathering indicators, suggesting that both the Sm-Nd and Lu-Hf systems are fairly robust against Antarctic weathering relative to the Rb-Sr system (Nishikawa *et al.*, 1990). However, the most weathered sample in this study, as indicated by the weathering index C and the lowest normalized Rb abundance (Table 5), A 09516 (H6), shows the largest absolute δ^{147}Sm/^{144}Nd values in this study and an atypical CI-normalized REE signature that is characterized by subchondritic values and a positive Eu anomaly (Figs. 2 and 7). Therefore, the Sm-Nd and Lu-Hf systems are generally unaffected by Antarctic weathering except in the case of anomalous CI-normalized REE abundances, as all samples except A 09516 (H6) display normal chondritic REE patterns and low δ^{147}Sm/^{144}Nd and δ^{176}Lu/^{177}Hf values.

4.1.2 Loss of REEs in A 09516 (H6)

As described above, A 09516 clearly underwent a significant degree of alteration, both mineralogically and chemically. Since this sample was analyzed in duplicate and the low elemental abundances are observed for this sample twice, significant sample losses during acid decomposition can be ruled out. Moreover, no other sample analyzed in this study exhibits such low abundances. Given that the weathering mechanism that affected A 09516 appears considerably more complicated than that of any other sample, this H6 chondrite is excluded from the previous discussions and is discussed here separately.

The low P and REE abundances and the P/Mg of A 09516 relative to the other HCs (Tables 4 and 5) may imply a loss of Ca-phosphates, known to take place during the alteration of eucrites in Antarctica (Mittlefehldt and Lindstrom, 1991). However, the characteristic LREE depletion and Ce anomaly typical for alteration of Antarctic eucrites are not observed A 09516 (Fig. 2). Considering the CI-normalized REE abundance in Ca-phosphates of HCs (Ebihara and Honda, 1983; Ward *et al.*, 2017), HCs that have lost Ca-phosphates should display lower CI-normalized LREE abundances relative to the heavy REE (HREE) abundances, which indicates that the CI-normalized REE abundances in A 09516 cannot be explained only by a loss of Ca-phosphates, as is the case for the weathered Antarctic eucrites (Mittlefehldt and Lindstrom, 1991). Normal chondritic Th and U abundances in A 09516 (Table 4 and Fig. 2) support that this sample did not lose considerable Ca-phosphate, simply because Th and U are also concentrated in Ca-phosphates of OCs (Pellas and Störzer, 1975; Crozaz, 1979). Generally, OCs, including HCs, contain chlorapatite and merrillite as Ca-phosphates (*e.g.*, Van Schmus, 1969). The CI-normalized REE abundances in merrillite are relatively flat, while those in chlorapatite are more enriched in LREEs than in HREEs in OCs (Crozaz *et al.*, 1989; Ward *et al.*, 2017). In addition, the Th and U abundances in merrillite are considerably lower (~3 ppm and ~0.3 ppm, respectively) than those in chlorapatite (~11 ppm and ~7.5 ppm, respectively) for OCs (Crozaz, 1974, 1979), implying that a loss of merrillite from bulk OCs affects the bulk Th and U abundances significantly less than a loss of chlorapatite. Thus, the REE abundances in A 09516 might be explained by the selective or more rapid dissolution of merrillite rather than chlorapatite during Antarctic alteration. However, the solubilities of merrillite and chlorapatite are comparable under acidic conditions (Adcock *et al.*, 2013), and selective or rapid dissolution of merrillite is hence unlikely. Therefore, a simple loss of Ca-phosphates by alteration cannot explain the elemental composition of A 09516.

Alternatively, chemical leaching depending on the solubility of an element, for example taking place at grain boundaries, could explain the elemental losses observed for A 09516. It is assumed that this mechanism does not strongly affect the mineralogy of the OCs, as highly mobile elements are leached more during this type of alteration. According to studies dealing with the mobility of REEs during weathering (Nesbitt, 1979; Middelburg *et al.*, 1988; van der Weijden and van der Weijden, 1995; Hannigan and Sholkovitz, 2001; Su *et al.*, 2017), the middle REEs (MREEs) and HREEs can more strongly be leached than the LREEs by alteration depending on the redox conditions, which could produce the observed REE abundances in A 09516. This can leave immobile elements such as Hf and Th in this sample. Moreover, the solubility difference explains the large deviation from the isochron on the Sm-Nd plots for A 09516 (Figs. 4 and 7) because any weathering mechanism affecting the modal abundance of the constituent minerals, such as a loss of Ca-phosphates, could not induce this divergence. However, the positive Eu anomaly in A 09516 cannot be produced by this leaching mechanism because the sample would exhibit no or rather a negative Eu anomaly if leaching occurred following their solubilities only. In addition, the Lu/Hf data in A 09516 display only a limited deviation (δLu/Hf = -1.32 ± 0.23 ‰; Figs. 5 and 7) from the isochron while the Sm-Nd data show a larger deviation (δSm/Nd = -5.58 ± 1.40 ‰ and -10.5 ± 1.4 ‰; Figs. 4 and 7), which is inconsistent with their relative mobility. Therefore, the chemical leaching depending on the solubility of an element can also not fully explain the characteristics of A 09516.

Lastly, two speculative possibilities remain to explain the REE abundances in A 09516: either some Ca-phosphates were partially leached during Antarctic alteration, or some Ca-phosphates were completely leached during Antarctic alteration, but the sample was at a later stage contaminated by terrestrial material. Similar scenarios have been proposed by Bast *et al*. (2017b) to explain the observed discrepancies from the reference isochron for bulk Lu-Hf data in eucrites and angrites. In the case of the former scenario, Ca-phosphates are fractured to some extent by an interruption in the ionic bonding between cations, especially impurity cations, and $(PO_4)^{2-}$ in the Ca-phosphates as the result of Antarctic alteration, but the Ca-phosphates are not completely broken due to insufficiencies in time, in the amount of fluid, or in the pH of the fluid during the leaching. This leads to selective leaching of more soluble trace elements from Ca-phosphates. In this case, the losses of MREEs and HREEs are more remarkable than those of LREEs, while the positive Eu anomaly and the normal Th and U abundances in A 09516 remain. Moreover, this incomplete dissolution of Ca-phosphates can produce the disturbance on the Sm-Nd plots for A 09516. However, the observation of a lack of disturbance for the Lu/Hf in A 09516 still remains to be explained. In the case of the latter scenario, contamination by terrestrial material during residence in Antarctica (Delisle *et al*., 1989; Welten *et al*., 2001) or during the experimental procedure such as sample crushing cannot be ruled out completely, although the contamination during Antarctic residence is unlikely because other samples, collected in the vicinity of A 09516, show no traces of contamination based on the results in this study. In both cases of contamination, some Ca-phosphates are removed by leaching during Antarctic alteration entirely, but the abundances of LREEs, Th, and U in A 09516 remain elevated because of terrestrial contamination. This can also explain the disturbance of Sm/Nd, the presence of the positive Eu anomaly and even the absence of any disturbance of the Lu/Hf because of less pronounced effects from terrestrial contamination on the Lu and Hf abundances. However, the observation that the Th and U abundances are still chondritic limits the possible admixture of terrestrial material. In any case, both possibilities including the loss of Ca-phosphates are inconsistent with a high modal abundance of Ca-phosphates in this sample (0.75 wt. %; Table 3), although their mass scales need to be considered. Therefore, A 09516 may have lost some amount of Ca-phosphates, but the way this HC lost Ca-phosphates appears to be different from how Antarctic eucrites are affected (Mittlefehldt and Lindstrom, 1991), indicating that Antarctic alteration may be significantly more complicated than what is expected based on heavily altered samples.

4.2 Control of heterogeneity on bulk Sm-Nd and Lu-Hf data by Ca-phosphates and Ca-pyroxene

The isotopic heterogeneity mostly depends on the sample heterogeneity unless the sample is affected by terrestrial weathering, as discussed above. Thus, it is important to constrain which minerals mainly affect the

Sm-Nd and Lu-Hf data of bulk chondrites. To do this, elemental abundance ratios in Antarctic HCs were compared with their isotope ratios, and their correlation coefficients r are shown in Table 6. If a constituent mineral controls the heterogeneity in bulk Sm-Nd and Lu-Hf data, elements accommodated in the mineral should display co-variation with the isotope data, if no selective removal or addition of elements occurred during weathering. According to the correlation coefficients for all samples, P/Mg and Y/Mg display strong positive correlations with ^{147}Sm/^{144}Nd, ^{176}Lu/^{177}Hf, and ^{176}Hf/^{177}Hf (r = 0.5-0.8) and strong negative correlations with ^{143}Nd/^{144}Nd (r = -0.6 and -0.7, respectively). If A 09516 (H6) is excluded, because its ^{147}Sm/^{144}Nd is the most disturbed by Antarctic weathering among the samples studied in this work, the P/Mg displays a strong negative correlation with ^{147}Sm/^{144}Nd instead of a positive correlation (r = -0.6; Table 6). In the case of OCs, Y is distributed in Ca-phosphates (*e.g.*, Mason, 1970), and Ca-phosphates have lower ^{147}Sm/^{144}Nd and ^{143}Nd/^{144}Nd values and higher ^{176}Lu/^{177}Hf and ^{176}Hf/^{177}Hf values compared to bulk samples (Amelin and Rotenberg, 2004; Amelin, 2005; Debaille *et al.*, 2017). Thus, these correlations indicate that the isotope ratios in bulk samples highly depend on the Ca-phosphates-to-silicates weight ratio in the sample, because the P/Mg and Y/Mg can be considered as indicators of the Ca-phosphates/silicates.

The correlation coefficients excluding A 09516 (H6) are shown in Table 6, not only because of the reasons outlined above but also because this sample is characterized by an abnormally low abundance of Ca-phosphates as discussed in the subsection 4.1.2. When A 09516 (H6) is excluded, the P/Mg no longer correlates with the ^{176}Lu/^{177}Hf and ^{176}Hf/^{177}Hf. Because the Y/Mg still correlates with these ratios and P is in part distributed in metals especially in unequilibrated chondrites (Murrell and Burnett, 1983; Zanda *et al.*, 1994), this may be caused by a disturbance of the bulk P abundance through the accommodation of P in metal. On the other hand, Al/Mg, Ca/Mg, and Ti/Mg display negative correlations with ^{176}Lu/^{177}Hf and ^{176}Hf/^{177}Hf (r = -0.8 to -0.4), although the correlations with Al/Mg are relatively weak (r = -0.4 and -0.5, respectively). According to *in-situ* analyses and Hf partition coefficients of minerals (Alexander, 1994; Righter and Shearer, 2003; Martin *et al.*, 2013), Hf is distributed in chondrule glass and Ca-pyroxene in unequilibrated chondrites and in Ca-pyroxene in equilibrated chondrites. Aluminum, Ca, and Ti are distributed in these silicate minerals as well, although Al is mostly distributed in feldspar in EOCs (Curtis and Schmitt, 1979; Alexander, 1994). Considering the REE distribution in EOCs, Lu is not only distributed in Ca-phosphates but also partitioned to a large degree into Ca-pyroxene, while Sm and Nd are mostly distributed in Ca-phosphates (*e.g.*, Curtis and Schmitt, 1979). In the case of UOCs, Lu is distributed in chondrule glass and Ca-pyroxene (Alexander, 1994; Shinotsuka, 1997). In addition, chondrule glass has the lowest Lu/Hf among silicates and Ca-phosphates for unequilibrated chondrites and Ca-pyroxene has the lowest Lu/Hf among these minerals for equilibrated chondrites (Alexander, 1994; Martin *et al.*, 2013). Therefore, the negative correlations of Al/Mg, Ca/Mg, and Ti/Mg with ^{176}Lu/^{177}Hf and ^{176}Hf/^{177}Hf indicate that the amount of Ca-pyroxene, which is a major host phase of Hf and a partial carrier of Lu, affects the heterogeneity of bulk Lu-Hf data. Moreover, the negative correlations are also produced by the heterogeneity in the amount of chondrule glass, which is a major host phase of Lu and Hf in UHCs. The negative correlation between Ti/Mg and Lu-Hf data may also be affected by the amount of ilmenite, which can have lower Lu/Hf than that in Ca-pyroxene according to their partition coefficients (Green, 1994; Kleine *et al.*, 2008). However, considering the budget of Hf between constituent minerals in the whole rock, the correlation mostly depends on the weight ratio of Ca-pyroxene to silicates (or Ca-pyroxene and chondrule glass to silicates).

According to Table 6, P/Ca and Y/Ca exhibit negative correlations with Sm-Nd data and positive correlations with Lu-Hf data, both when including and excluding A 09516 (H6), although ^{147}Sm/^{144}Nd still displays positive correlations possibly because of the disturbance by weathering. Most of these correlations are stronger than those for the P/Mg and Y/Mg. For OCs, REEs including Y are mostly distributed among the two phases of Ca-phosphate and Ca-pyroxene (Ehihara and Honda, 1984). Among silicates and Ca-phosphates in chondrites, Ca-phosphates have the highest P/Ca, Y/Ca, and Lu/Hf and the lowest Sm/Nd (*e.g.*, Curtis and Schmitt, 1979; Amelin, 2005). In contrast, Ca-pyroxene has the lowest P/Ca, Lu/Hf, and Y/Ca and the highest or second highest Sm/Nd (Curtis and Schmitt, 1979; Alexander, 1994; Martin *et al.*, 2013). Thus, Ca-phosphates and Ca-pyroxene are considered to be the endmembers of the bulk P/Ca, Y/Ca, Sm/Nd, and Lu/Hf, indicating that the correlations of the P/Ca and Y/Ca reflect the Ca-phosphates-to-Ca-pyroxene weight ratio. Therefore, the heterogeneity of Sm-Nd and Lu-Hf data in bulk OCs is mainly controlled by the weight ratio of Ca-phosphates to Ca-pyroxene in the sample. For UOCs, the amount of chondrule glass also affects the overall REE budget and isotopic values.

4.3 Relationship between the distributions of REEs and Hf and the heterogeneities of bulk Sm-Nd and Lu-Hf data

According to the result of the *in-situ* measurement in this study, the modal abundance of Ca-phosphates in UHCs is significantly lower than that in EHCs (Fig. 1). This increase in the modal abundances of Ca-phosphates from UHCs to EHCs must result from thermal metamorphism on their parent body(ies) (Huss *et al.*, 2006). On the other hand, the bulk REE and P abundances overlap within uncertainty between UHCs and EHCs, which is consistent with previous works (*e.g.*, Jarosewich, 1990). Murrell and Burnett (1983) reported that Ca-phosphate grains in UOCs are very fine (< 10 μm). Perron *et al.* (1992) found phosphate, chromite, silica, and silica inclusions as secondary minerals in some UOCs. However, Semarkona (LL3.00), which is one of the least metamorphosed chondrites, does not contain such grains. Based on these observations, combining the bulk P abundances and the modal abundances of Ca-phosphates between UHCs and EHCs used in this study, Ca-phosphates must have formed and grown in a closed system during thermal metamorphism on the parent body or bodies. Ebihara (1989) and Shinotsuka (1997) analyzed REE abundances in acid residues of OCs with lower and higher degrees of metamorphism, which were leached using HCl or HNO_3. Because REEs are enriched in chondrule glass in UOCs (Alexander, 1994), Shinotsuka (1997) suggested that the REEs are re-distributed mainly from chondrule glass to Ca-phosphates during thermal metamorphism. Since the bulk REE abundances are the same between UOCs and EOCs, the re-distribution of REEs may have occurred in a closed system with the growth of Ca-phosphates. This REE re-distribution in a closed system can explain the observation that the Sm-Nd and Lu-Hf data of each constituent mineral in chondrites are plotted on the respective chondrite isochrons (Amelin and Rotenberg, 2004; Amelin, 2005; Debaille *et al.*, 2017). In this way, because REEs are more distributed to Ca-phosphates in EOCs than UOCs, the nugget effect of Ca-phosphates for EOCs produces larger isotopic variabilities of Sm-Nd and Lu-Hf systematics than that for UOCs, which reinforces the conclusions by Bouvier *et al.* (2008) and Dauphas and Pourmand (2011, 2015). Moreover, sampling effects on bulk Lu-Hf data due to a heterogeneous distribution of Ca-pyroxene may be larger in EOCs than in UOCs because Lu is hosted in Ca-pyroxene as well as Ca-phosphates, while Hf seems to be re-distributed from chondrule glass to Ca-pyroxene based on their initial distribution and their re-distribution after metamorphism (Curtis and Schmitt, 1979; Alexander, 1994; Righter and Shearer, 2003; Martin *et al.*, 2013), although no data exist on the Hf distribution in OCs and the mobility of Hf during thermal metamorphism. These larger contributions to bulk Sm-Nd and Lu-Hf data by the sampling heterogeneities of Ca-phosphates and Ca-pyroxene in EOCs in terms of the distributions of REE and Hf are complementary to the correlations between the elemental abundance ratios and the isotopic ratios obtained in this study (Table 6). Therefore, unequilibrated chondrites in which the re-distributions have not proceeded in the case of OCs should be used for the determination of precise average Sm-Nd and Lu-Hf isotopic compositions to limit the effects of the sampling heterogeneities, reinforcing the conclusions by Bouvier *et al.* (2008) and Debaille *et al.* (2017). Even in this case, the sampling heterogeneity of chondrule glass can still lead to heterogeneity in the bulk Sm-Nd and Lu-Hf data although the effect on the isotope data by the heterogeneous distribution of chondrule glass appears to be less than that by the heterogeneous distribution of Ca-phosphates. Theoretically, equilibrated chondrites could also be useful for the determination of precise average isotopic compositions as aimed for the CHUR values if a sufficiently large amount of the sample is homogenized (speculatively more than a few grams at least), because the heterogeneity of bulk Sm-Nd and Lu-Hf data only results from the sample heterogeneity, provided that re-distributions occurred in a closed system. Based on Patchett *et al.* (2004) and Bouvier *et al.* (2008), the mean values and uncertainties of bulk Sm-Nd data in equilibrated chondrites are almost the same as those in unequilibrated chondrites when a few grams of equilibrated chondrite are homogenized (^{147}Sm/^{144}Nd = 0.1960 ± 0.0006 and 0.1960 ± 0.0004; ^{143}Nd/^{144}Nd = 0.512634 ± 0.000012 and 0.512630 ± 0.000011, respectively) On the other hand, the homogenization with even a few grams of equilibrated chondrite seems to be insufficient for the determination of bulk average Lu-Hf isotopic compositions for the purpose of CHUR determination (^{176}Lu/^{177}Hf = 0.0324 ± 0.0009 and 0.0336 ± 0.0001; ^{176}Hf/^{177}Hf = 0.282693 ± 0.000078 and 0.282785 ± 0.000011, the same order as above), as also concluded by Patchett *et al.* (2004). Thus, equilibrated chondrites may provide representative Sm-Nd isotopic compositions in individual samples as long as more than a few grams of the sample is homogenized to remove the nugget effect, and such data would be useful for the determination of precise average Sm-Nd isotopic compositions for individual chondrite groups. However, because of the uncertainty related to the essential mass to be actually representative, only unequilibrated chondrites should be used for the determination of the precise Lu-Hf CHUR values, probably applied to the determination of precise average Sm-Nd isotopic compositions for individual chondrite groups as well. This difference in sufficient sample amounts for homogenization may be because the variation in Sm-Nd data largely depends on the sampling heterogeneity of Ca-phosphates, while the variation in Lu-Hf data depends not only on the sampling heterogeneity of Ca-phosphates but also on that of Ca-pyroxene and chondrule glass.

The distributions of REEs and Hf and the redistribution of these elements during parent body processes differ between the various classes of chondrites as the major hosts of those elements and their parent body processes vary, as shown in Table 7, although the distribution and the mobility of Hf remain poorly understood. Sampling biases involving these major hosts are largely responsible for the observed variations in Sm-Nd and Lu-Hf isotopic ratios. For example, CV and CO chondrites contain abundant Ca, Al-rich inclusions (CAIs; 2.98 vol.% and 0.99 vol.%, respectively; Hezel *et al.*, 2008), producing variable REE abundances and probably variable Hf abundance as well, as the result of a heterogeneous distribution of CAIs in samples of these meteorites. However, CI-normalized abundances of REEs in bulk CAIs are only ~20×CI (*e.g.*, El Goresy *et al.*, 2002), while bulk oldhamite in enstatite chondrites and bulk Ca-phosphates in R chondrites contain ~100×CI and ~200×CI of REEs, respectively (Laimer and Ganapathy, 1987; Maeda *et al.*, 2017a). Moreover, other refractory components such as amoeboid olivine aggregates contain much less REE and Hf abundances (Krot *et al.*, 2004). Thus, based on mass balance considerations, the nugget effects of CAIs or other refractory components on the Sm-Nd and Lu-Hf isotopic heterogeneities are not as much as those of Ca-phosphates or oldhamite. In the cases of enstatite and Rumuruti chondrites, the modal abundances of the REE host phases are only less than 2 wt. % and about 0.4 wt. %, respectively (Crozaz and Lundberg, 1995; Bischoff *et al.*, 2011). Moreover, Barrat *et al.* (2014) and Maeda *et al.* (2017b) concluded that the REEs of both chondrite types were re-distributed between the respective host phases during thermal metamorphism. Thus, similar to OCs, the unequilibrated counterparts of these other chondrite classes should be preferred to determine the precise average Sm-Nd and Lu-Hf isotopic compositions for enstatite and Rumuruti chondrites to avoid strong nugget effects of the respective host phases. This may also apply to CK chondrites because these experienced thermal metamorphism and contain < 1 vol. % of Ca-phosphates as one of the hosts of REEs (Martin *et al.*, 2013). Kakangari, CV, and CO chondrites underwent aqueous alteration but simultaneously also underwent a limited degree of thermal metamorphism on their parent bodies. However, their thermal metamorphism occurred within the unequilibrated range, implying the effect of elemental re-distribution by thermal metamorphism is almost negligible. For many groups of carbonaceous chondrites that underwent aqueous alteration, it is unclear whether heavily altered samples can be used for the determination of the precise average isotopic compositions because the redistribution of REEs and Hf during aqueous alteration remains poorly constrained. According to Bouvier *et al.* (2008), aqueously altered samples produce fewer heterogeneities of bulk Sm-Nd and Lu-Hf data than metamorphosed samples. Therefore, the use of unequilibrated chondrites not only for OCs but also for most other classes of chondrites can reduce the effect of variability in the isotope data stemming from the sample heterogeneity, which is required for the determination of precise average Sm-Nd and Lu-Hf isotopic compositions for individual chondrite groups.

5 CONCLUSIONS

In this study, we analyzed ten Antarctic HCs and three HCs from hot deserts in a systematic manner to determine their modal mineral abundances, major and trace elemental abundances, and Sm-Nd and Lu-Hf isotopic compositions. The following conclusions can be drawn.

Firstly, by calculating the Rb abundances normalized to the average Na and Al abundances for each sample to evaluate Antarctic chemical alteration, our results indicate that not all weathered samples categorized as C according to the weathering index display a loss of Rb. Conversely, samples categorized as A/B may exhibit a high Rb loss. Thus, the normalized Rb abundance can be a good indicator for the assessment of Antarctic alteration chemically but only indicates the relative intensity of the chemical weathering in Antarctica.

Secondly, the effects of Antarctic alteration on the Sm-Nd and Lu-Hf systems in bulk HCs are evaluated using the δ^{147}Sm/^{143}Nd and δ^{176}Lu/^{177}Hf notations. These values do not correlate with the weathering index or the Rb indicator, except in the case of a single heavily weathered sample A 09516 (H6), which displays various element losses, including for the REEs. This result suggests that the Sm-Nd and Lu-Hf systems preserve their original compositions during Antarctic alteration. However, when a sample is heavily affected by Antarctic weathering and has lost many elements, the isotope systems may also be disturbed. Such high elemental losses might reflect partial dissolution of Ca-phosphates during alteration. Therefore, unless the sample is clearly heavily weathered, most Antarctic meteorites, including rare meteorites such as ungrouped, shergottites-nakhlites-chassignites, and lunar meteorites can be used for the investigation of their Sm-Nd and Lu-Hf isotopic compositions.

Finally, we confirm that the Sm-Nd and Lu-Hf data in bulk HCs are correlated with the weight ratio of Ca-phosphates to silicates. The weight ratio of Ca-phosphates to Ca-pyroxene may correlate stronger with the isotopic ratios, especially in the case of the Lu-Hf system. Sample heterogeneity of Ca-phosphates in HCs may thus lead to heterogeneities in the bulk Sm-Nd and Lu-Hf data. Since REEs in OCs are re-distributed to Ca-phosphates in a closed system during thermal metamorphism on the parent body(ies), the nugget effect of Ca-phosphates on the heterogeneities of bulk Sm-Nd and Lu-Hf isotope data is larger for EOCs than for UOCs. Therefore, the use of UOCs should be preferred for the determination of well-constrained average Sm-Nd and Lu-Hf isotopic compositions such as CHUR values unless at least a few grams of EOCs are used, which reinforces the conclusion by Bouvier *et al*. (2008). The preferred use of unequilibrated specimens may also be extended to the other classes of chondrites, but the optimal sample amount for homogenization to obtain representative Sm-Nd and Lu-Hf isotopic compositions in a sample is expected to differ for each class because the host phases of REEs and Hf and their remobilization during parent body processes are distinct. For the analysis of bulk isotope data, major and trace elemental abundances should be determined together with the isotope data in order to evaluate the sample heterogeneity and to assess the effects of weathering. A better understanding of the Hf distribution on the bulk meteorite scale, the Hf mobilization during thermal metamorphism, and the redistribution of REEs and Hf during aqueous alteration on meteorite parent bodies may help to determine the sample sizes required to overcome sample heterogeneity and to measure representative Sm-Nd and Lu-Hf isotopic compositions in individual samples, leading to precise average Sm-Nd and Lu-Hf isotopic compositions for individual chondrite groups.

Acknowledgments

We would like to thank S. Cauchies and W. Debouge for assistance in the lab, J. De Jong for helping with the isotope analysis, and N. J. de Winter for guidance with the µXRF. We also thank the Royal Belgian Institute of Natural Sciences, Belgium, and the National Institute of Polar Research, Japan, for the loan of the Antarctic meteorites and meteorites collected from hot deserts used in this study. RM, SG, VD and PhC acknowledge support from the Excellence of Science (EoS) project “ET-HoME”. SG, VD and GH thank the BRAIN-Be Belgian Science Policy (BELSPO) project “BAMM”. VD thanks the ERC StG ISoSyC and FRS-

FNRS for support. HP acknowledges receiving funding from the European Union's Horizon 2020 research and innovation program under the Marie Skłodowska-Curie grant agreement No 801505. PhC acknowledges support from the VUB Strategic Research Program and the Research Foundation Flanders (FWO Hercules grant) for the purchase of the µXRF instrument. Finally, we are grateful to Audrey Bouvier for her editorial work and insightful comments during the review process. We also thank Erik Scherer, Minako Righter, and an anonymous reviewer for their constructive and detailed reviews.

REFERENCES

Adcock C. T., Hausrath E. M. and Forster P. M. (2013) Readily available phosphate from minerals in early aqueous environments on Mars. *Nat. Geosci.* **6**, 824-827.

Alexander C. M. O'D. (1994) Trace element distributions within ordinary chondrite chondrules: Implications for chondrule formation conditions and precursors. *Geochim. Cosmochim. Acta* **58**, 3451-3468.

Al-Kathiri A., Hofmann B. A., Jull J. T. and Gnos E. (2005) Weathering of meteorites from Oman: Correlation of chemical and mineralogical weathering proxies with ^{14}C terrestrial ages and the influence of soil chemistry. *Meteorit. Planet. Sci.* **40**, 1215-1239.

Amelin Y. (2005) Meteorite phosphates show constant ^{176}Lu decay rate since 4557 million years ago. *Science* **310**, 839-841.

Amelin Y. and Rotenberg E. (2004) Sm–Nd systematics of chondrites. *Earth Planet. Sci. Lett.* **223**, 267-282.

Anders E. and Grevesse N. (1989) Abundances of the elements: Meteoritic and solar. *Geochim. Cosmochim. Acta* **53**, 197-214.

Armytage R. M. G., Debaille V., Brandon A. D. and Agee C. B. (2018) A complex history of silicate differentiation of Mars from Nd and Hf isotopes in crustal breccia NWA 7034. *Earth and Planet. Sci. Lett.* **502**, 274-283.

Barosch J., Ebel D.S., Hezel D. C., Alpert S. and Palme H. (2020) Formation of chondrules and matrix in Kakangari chondrites. *Earth and Planet. Sci. Lett.* **542**, 116286.

Barrat J. A., Zanda B., Jambon A. and Bollinger C. (2014) The lithophile trace elements in enstatite chondrites. *Geochim. Cosmochim. Acta* **128**, 71-94.

Bast R., Scherer E. E. and Bischoff A. (2017a) The ^{176}Lu-^{176}Hf systematics of ALM-A: A sample of the recent Almahata Sitta meteorite fall. *Geochem. Pers. Lett.* **3**, 45–54.

Bast R., Scherer E. E., Sprung P., Mezger K., Fischer-Gödde M., Taetz S., Böhnke M., Schmid-Beurmann H., Münker C., Kleine T. and Srinivasan G. (2017b). Reconciliation of the excess ^{176}Hf conundrum in meteorites: Recent disturbances of the Lu-Hf and Sm-Nd isotope systematics. *Geochim. Cosmochim. Acta* **212**, 303–323.

Bischoff A., Vogel N. and Roszjar J. (2011) The Rumuruti chondrite group. *Chemie der Erde* **71**, 101-133.

Bizzarro M., Baker J. A., Haack H., Ulfbeck D. and Rosing, M. (2003) Early history of the Earth's crust–mantle system inferred from hafnium isotopes in chondrites. *Nature* **421**, 931-933.

Bland P. A., Zolensky M. E., Benedix G. K. and Sephton M. A. (2006) Weathering of chondritic meteorites. In *Meteorites and the Early Solar System II* (eds. Lauretta D. S. and McSween Jr. H. Y.). The University of Arizona Press, Tucson, pp. 853-867. in collaboration with Lunar and Planetary Institute, Houston.

Blichert-Toft J. and Albarède F. (1997) The Lu–Hf isotope geochemistry of chondrites and the evolution of the mantle–crust system. *Earth Planet. Sci. Lett.* **148**, 243-258.

Blichert-Toft J., Chauvel C. and Albarède F. (1997) Hf and Lu for high-precision isotope analysis of rock samples by magnetic sector-multiple collector ICP-MS. *Contrib. Mineral. Petrol.* **127**, 248-260.

Bloch E., Watkins J. and Ganguly J. (2017) Diffusion kinetics of lutetium in diopside and the effect of thermal metamorphism on Lu–Hf systematics in clinopyroxene. *Geochim. Cosmochim. Acta* **204**, 32-51.

Bloch E., Watkins J. and Ganguly J. (2018) Comment on "Reconciliation of the excess 176Hf conundrum in meteorites: Recent disturbances of the Lu-Hf and Sm-Nd isotope systematics" [Geochim. Cosmochim. Acta 212 (2017) 303–323]. *Geochim. Cosmochim. Acta* **230**, 190-192.

Bouvier A., Vervoort J. D. and Patchett P. J. (2008) The Lu–Hf and Sm–Nd isotopic composition of CHUR: Constraints from unequilibrated chondrites and implications for the bulk composition of terrestrial planets. *Earth Planet. Sci. Lett.* **273**, 48-57.

Burkhardt C., Borg L. E., Brennecka G. A., Shollenberger Q. R., Dauphas N. and Kleine T. (2016) A nucleosynthetic origin for the Earth's anomalous ^{142}Nd composition. *Nature* **537**, 394-398.

Boyet M. and Carlson R. W. (2005) Chondrite barium, neodymium, and samarium isotopic heterogeneity and early Earth differentiation. *Science* **316**, 1175-1178.

Carlson R. W., Boyet M. and Horan M. (2007) ^{142}Nd evidence for early (>4.53 Ga) global differentiation of the silicate. *Science* **309**, 576-581.

Chauvel C. and Blichert-Toft J. (2001) A hafnium isotope and trace element perspective on melting of the depleted mantle. *Earth Planet. Sci. Lett.* **190**, 137-151.

Crozaz G. (1974) U, Th and extinct ^{244}Pu in the phosphates of the St. Severin meteorite. *Earth Planet. Sci. Lett*. **23**, 164-169.

Crozaz G. (1979) Uranium and thorium microdistributions in stony meteorites. *Geochim. Cosmochim. Acta* **43**, 127-136.

Crozaz G. and Lundberg L. L. (1995) The origin of oldhamite in unequilibrated enstatite chondrites. *Geochim. Cosmochim. Acta* **59**, 3817-3831.

Crozaz G., Pellas P., Bourot-Denise M., de Chazal S. M., Fieni C., Lundberg L. L. and Zinner E. (1979) Plutonium, uranium and rare earths in the phosphates of ordinary chondrites—The quest for a chronometer. *Earth Planet. Sci. Lett.* **93**, 157-169.

Crozaz G., Floss C. and Wadhwa M. (2003) Chemical alteration and REE mobilization in meteorites from hot and cold deserts. *Geochim. Cosmochim. Acta* **67**, 4727-4741.

Curtis D. B. and Schmitt R. A. (1979) The petrogenesis of L-6 chondrites: insights from the chemistry of minerals. *Geochim. Cosmochim. Acta* **43**, 1091-1103.

Dauphas N. and Pourmand A. (2011) Hf–W–Th evidence for rapid growth of Mars and its status as a planetary embryo. *Nature* **473**, 489.

Dauphas N. and Pourmand A. (2015) Thulium anomalies and rare earth element patterns in meteorites and Earth: Nebular fractionation and the nugget effect. *Geochim. Cosmochim. Acta* **163**, 234-261.

Davis A. M. (2006) Volatile evolution and loss. In *Meteorites and the Early Solar System II* (eds. Lauretta D. S. and McSween Jr. H. Y.). The University of Arizona Press, Tucson, pp. 295–307. in collaboration with Lunar and Planetary Institute, Houston.

Debaille V., Brandon A. D. Yin Q. Z. and Jacobsen B. (2007) Coupled ^{142}Nd–^{143}Nd evidence for a protracted magma ocean in Mars. *Nature* **450**, 525-528.

Debaille V., Orman J. V., Yin Q. Z. and Amelin Y. (2017) The role of phosphates for the Lu–Hf chronology of meteorites. *Earth Planet. Sci. Lett.* **473**, 52-61.

Delisle G., Schultz L., Spettel B., Weber H. W., Wlotzka F., Hofle H. C., Thierbach R., Vogt S., Herpers U., Bonani G. and Suter M. (1989) Meteorite finds near the Frontier Mountain Range in North Victoria Land. *Geol. Jb.* **38**, 483-513.

DePaolo D. J. and Wasserburg G. J. (1976) Nd isotopic variations and petrogenetic models. *Geophys. Res. Lett*. **3**, 249–252.

Ebihara M. (1987) Determination of ten lanthanoids in chondritic meteorites by radiochemical neutron activation analysis using coaxial and planar type pure Ge detectors. *J. Radioanal. Nucl. Chem.* **111**, 385-397.

Ebihara M. (1988) Trace element composition and distribution of Yamato-691, an unequilibrated enstatite chondrite. *Proc. NIPR Symp. Antract. Meteorites* **1**, 102-112.

Ebihara M. (1989) Rare earth and some other elements in acid-residues od unequilibrated ordinary chondrites. *Proc. NIPR Symp. Antract. Meteorites* **2**, 279-287.

Ebihara M., Hayano K. and Shirai N. (2020) Determination of trace rare earth elements in rock samples including meteorites by ICP-MS coupled with isotope dilution and comparison methods. *Anal. Chim. Acta* **1101**, 81-89.

Ebihara M. and Honda M. (1983) Rare earth abundances in chondritic phosphates and their implications for early stage chronologies. *Earth and Planet. Sci. Lett.* **63**, 433-445.

Ebihara M. and Honda M. (1984) Distribution of rare earth elements and uranium in various components of ordinary chondrites. *Meteoritics* **19**, 69-77.

Ebihara M. and Honda M. (1987) Rare earth elements in Ca-phosphates of Allende carbonaceous chondrite. *Meteoritics* **3**, 179-190.

El Goresy A., Zinner E., Matsunami S., Palme H., Spettel B., Lin Y. and Nazarov M. (2002) Efremovka 101.1: A CAI with ultrarefractory REE patterns and enormous enrichments of Sc, Zr, and Y in Fassaite and Perovskite. *Geochim. Cosmochim. Acta* **66**, 1459-1491.

Fukai R. and Yokoyama T. (2017) Neodymium isotope heterogeneity of ordinary and carbonaceous chondrites and the origin of non-chondritic ^{142}Nd compositions in the Earth. *Earth Planet. Sci. Lett.* **474**, 206-214.

Gannoun A., Boyet M., Rizo H. and El Goresy A. (2011) ^{146}Sm–^{142}Nd systematics measured in enstatite chondrites reveals a heterogeneous distribution of ^{142}Nd in the solar nebula. *Proc. Natl. Acad. Sci.* **108**, 7693-7697.

Goderis S., Yesiltas M., Pourkhorsandi H., Shirai N., Poudelet M., Martin L., Yamaguchi A., Debaille V. and Claeys Ph. (2021) Detailed record of the BELARE 2019-2020 meteorite recovery expedition on the Nansen Ice Field, East Antarctica. *Antarctic Record* **65**, 1-20.

Green T. H. (1994) Experimental studies of trace-element partitioning applicable to igneous petrogenesis — Sedona 16 years later. *Chem. Geol.* **117**, 1-36.

Hannigan R. E. and Sholkovitz E. R. (2001) The development of middle rare earth element enrichments in freshwaters: Weathering of phosphate minerals. *Chem. Geol.* **175**, 495-508.

Hezel D. C., Russell S. S., Ross A. J. and Kearsley A. T. (2008) Modal abundances of CAIs: Implications for bulk chondrite element abundances and fractionations. *Meteorit. Planet. Sci.* **43**, 1879-1894

Hublet G., Yamaguchi A., Debaille V., Shirai N. and Kimura M. (2019) Geochemical study of type 3 ordinary chondrites. In *the 82nd Ann. Mtg. Met. Soc.*, #6257. LPI Contribution No. 2157, Lunar and Planetary Institute, Houston (abstract).

Huss G. R., Rubin A. E. and Grossman J. N. (2006) Thermal metamorphism in chondrites. In *Meteorites and the Early Solar System II* (eds. Lauretta D. S. and McSween Jr. H. Y.). The University of Arizona Press, Tucson, pp. 567–586. in collaboration with Lunar and Planetary Institute, Houston.

Jacobsen S. B. and Wasserburg G. J. (1980) Sm–Nd isotopic evolution of chondrites. *Earth Planet. Sci. Lett.* **50**, 139-155.

Jacobsen S. B. and Wasserburg G. J. (1984) Sm–Nd isotopic evolution of chondrites and achondrites, II. *Earth Planet. Sci. Lett.* **67**, 137-150.

Jarosewich E. (1990) Chemical analyses of meteorites: A compilation of stony and iron meteorite analyses. *Meteoritics* **25**, 323-337.

Jochum M. P., Weis U., Scwager B., Stoll B, Wilson S. A., Haug G. H., Andreae M. O. and Enzweiler J. (2016) Reference values following ISO guidelines for frequently requested rock reference materials. *Geostand. Geoanal. Res.* **40**, 333-350.

Kleine T., Touboul M., Van Orman J. A., Bourdon B., Maden C., Mezger K. and Halliday A. (2008) Hf–W thermochronometry: closure temperature and constraints on the accretion and cooling history of the H chondrite parent body. *Earth Planet. Sci. Lett.* **270**, 106–118

Koebel C. and Cassidy W. (1991) Differences between Antarctic and non-Antarctic meteorites: An assessment. *Geochim. Cosmochim. Acta* **55**, 3-18.

Krot A. N., Keil K., Scott E. R. D., Goodrich C. A. and Weisberg M. K. (2003) Classification of meteorites. In *Meteorites, Comets, and Planets*, Treatise on Geochemistry (ed. Davis A. M.). Elsevier, Amsterdam, vol. 1, chap. 1.05, pp. 83-128.

Krot A. N., Petaev M. I., Russell S. S., Itoh S., Fagan T. J., Yurimoto H., Chizmadia L., Weisberg M. K., Komatsu M., Ulyanov A. A. and Keil K. (2004) Amoeboid olivine aggregates and related objects in carbonaceous chondrites: records of nebular and asteroid processes. *Chemie der Erde* **64**, 185-239.

Larimer J. W. and Ganapathy R. (1987) The trace element chemistry of CaS in enstatite chondrites and some implications regarding its origin. *Earth and Planet. Sci. Lett.* **84**, 123-134.

Lugmair G. W. and Marti K. (1978) Lunar initial ^{143}Nd/^{144}Nd: differential evolution of the lunar crust and mantle. *Earth Planet Sci. Lett.* **39**, 349-357.

Maeda R., Shirai N. and Ebihara M. (2017a) Distribution of rare earth elements, Th and U in R chondrite. In *Lunar Plant. Sci.* **XLVIII**, #2370. Lunar and Planetary Institute, Houston (abstract).

Maeda R., Shirai N., Yamaguchi A. and Ebihara M. (2017b) Formation process and metamorphism on R chondrite parent body based on distribution of rare earth elements, Th and U. In *The Eighth Symposium on Polar Science*, #00258. National Institute of Polar Science, Tokyo (abstract).

Martin C., Debaille V., Lanari P., Goderis S., Vandendael I., Vanhaecke F., Vidal O. and Claeys Ph. (2013) REE and Hf distribution among mineral phases in the CV–CK clan: A way to explain present-day Hf isotopic variations in chondrites. *Geochim. Cosmochim. Acta* **120**, 496-513.

Mason B. and Graham A.L. (1970) Minor and trace elements in meteoritic minerals. *Smithson. Contrib. Earth Sci.* **3**, 1-17.

McSween Jr. H. Y., Bennett III M. E. and Jarosewich E. (1991) The mineralogy of ordinary chondrites and implications for asteroid spectroscopy. *Icarus* **90**, 107-116.

Middelburg J. J., van der Weijden C. H. and Woittiez J. R. W. (1988) Chemical processes affecting the mobility of major, minor and trace elements during weathering of granitic rocks. *Chem. Geol.* **68**, 253-273.

Mittlefehldt D. W. and Lindstrom M. M. (1991) Generation of abnormal trace element abundances in Antarctic eucrites by weathering processes. *Geochim. Cosmochim. Acta* **55**, 77-87.

Murrell M. T. and Burnett D. S. (1983) The behavior of actinides, phosphorus, and rare earth elements during chondrite metamorphism. *Geochim. Cosmochim. Acta* **47**, 1999-2014.

Nakamura N. (1974) Determination of REE, Ba, Fe, Mg, Na and K in carbonaceous and ordinary chondrites. *Geochim. Cosmochim. Acta* **38**, 757-775.

Nesbitt H. W. (1979) Mobility and fractionation of rare earth elements during weathering of a granodiorite. *Nature* **279**, 206-210.

Nishiizumi K., Elmore D. and Kubik P. W. (1989) Update on terrestrial ages of Antarctic meteorites. *Earth Planet. Sci. Lett.* **93**, 299-313.

Nishikawa Y., Nakamura N., Misawa K., Okano O., Kagami H. and Yamamoto K. (1990) Investigation of the Weathering Effect on Rb-Sr Systematics and Trace Element Abundances in Antarctic and Non-Antarctic Meteorites: A Case of H-Chondrites. *Mass Spectrosc.* **38**, 115-123.

Patchett P. J., Vervoort J. D., Soderlund U. and Salters V. J. M. (2004) Lu–Hf and Sm–Nd isotopic systematics in chondrites and their constraints on the Lu–Hf properties of the Earth. *Earth Planet. Sci. Lett.* **222**, 29-41.

Pellas P. and Störzer D. (1975) Uranium and plutonium in chondritic phosphates. *Meteoritics* **10**, 471 (abstract).

Perron C., Zanda B., Bourot-Denise M., and Mostefaoui S. (1992) Bishunpur and Semarkona: New clues to the origin of inclusions in metal. *Meteoritics* **27**, 275-276.

Pourkhorsandi H., D'Orazio M., Rochette P., Valenzuela M., Gattacceca J., Mirnejad H., Sutter B., Hutzler A. and Aboulahris M. (2017) Modification of REE distribution of ordinary chondrites from Atacama (Chile) and Lut (Iran) hot deserts: Insights into the chemical weathering of meteorites. *Meteorit. Planet. Sci.* **52**, 1843-1858.

Pourkhorsandi H., Gattacceca J., Rochette P., D’Orazio M., Kamali H., de Avillez R., Letichevsky S., Djamali M., Mirnejad H., Debaille V. and Jull A.J.T. (2019) Meteorites from the Lut Desert (Iran). *Meteorit. Planet. Sci.* **54**, 1737-1763.

Pourkhorsandi H., Debaille V., Armytage R. M. G., van Ginneken M., Rochette P. and Gattacceca J. (2021) The effects of terrestrial weathering on samarium-neodymium isotopic composition of ordinary chondrites.

Chem. Geol. **562**, 120056.

Righter K. and Shearer C.K. (2003) Magmatic fractionation of Hf and W: Constraints on the timing of core formation and differentiation in the Moon and Mars. *Geochim. Cosmochim. Acta* **67**, 2497-2507.

Shima M. (1979) The abundances of titanium, zirconium and hafnium in stony meteorites. *Geochim. Cosmochim. Acta* **43**, 353-362.

Shima M. and Honda M. (1967) Distributions of alkali, alkaline earth and rare earth elements in component minerals of chondrites. *Geochim. Cosmochim. Acta* **31**, 1995-2006.

Shimizu H., Masuda A. and Tanaka T. (1983) Cerium anomaly in REE pattern of Antarctic eucrite. *Mem. Nat. Inst. Polar Res, Tokyo. Spec Issue* **30**, 341-348.

Shinotsuka K. (1997) Abundances of rare earth elements, thorium and uranium in chondritic meteorites. Ph. D. Thesis, Tokyo Metropolitan University, Tokyo, Japan. DOI: 10.11501/3126008.

Stöffler D., Keil K. and Scott E. R. D. (1991) Shock metamorphism of ordinary chondrites. *Geochim. Cosmochim. Acta* **55**, 3845-3867.

Su N., Yang S. Y., Guo Y. L., Yue W., Wang X. D., Yin P. and Huang X. T. (2017) Revisit of rare earth element fractionation during chemical weathering and river sediment transport. *Geochem. Geophys. Geosyst.* **18**, 935-955.

Tatsumoto M., Knight R. J. and Allegre C. J. (1973) Time Differences in the Formation of Meteorites as Determined from the Ratio of Lead-207 to Lead-206. *Science* **180**, 1279-1283.

Tatsumoto M., Unruh D. M. and Patchett P. J. (1981) U-Pb and Lu-Hf systematics of Antarctic meteorites. *Mem. Nat. Inst. Polar Res, Tokyo. Spec Issue* **20**, 237-249.

Taylor S. R. and McLennan S. M. (1995) The geochemical evolution of the continental crust. *Rev. Geophys.* **33**, 241-265.

van der Weijden C. H. and van der Weijden R. D. (1995) Mobility of major, minor and some redox-sensitive trace elements and rare-earth elements during weathering of four granitoids in central Portugal. *Chem. Geol.* **125**, 149-167.

Van Schmus W. R. (1969) The mineralogy and petrology of chondritic meteorites. *Earth Sci. Rev.* **5**, 145-184.

Velbel M. A. (1988) The distribution and significance of evaporitic weathering products on Antarctic meteorites. *Meteoritics* **23**, 151-159.

Velbel M. A., Long D. T. and Gooding J. L. (1991) Terrestrial weathering of Antarctic stone meteorites: Formation of Mg-carbonates on ordinary chondrites. *Geochim. Cosmochim. Acta* **55**, 67-76.

Ward D., Bischoff A., Roszjar J. and Whitehouse M. J. (2017) Trace element inventory of meteoritic Ca-phosphates. *American Mineralogist*, **102**, 1856-1880.

Wasson J. T. and Kallemeyn G. W. (1988) Compositions of chondrites. *Philos. Trans. R. Soc. Lond.*, A **325**, 535-544.

Weis D., Kieffer B., Maerschalk C., Barling J., de Jong J., Williams G. A., Hanano D., Pretorius W., Mattielli N., Scoates J. S., Goolaerts A., Friedman R. M. and Mahoney J. B. (2006) High-precision isotopic characterization of USGS reference materials by TIMS and MC-ICP-MS. *Geochem. Geophys. Geosyst.* **7**, Q08006.

Weis D., Kieffer B., Hanano D., Silva I. N., Barling J., Pretorius W., Maerschalk C. and Mattielli N. (2007) Hf isotope compositions of US Geological Survey reference materials. *Geochem. Geophys. Geosyst.* **8**, Q06006.

Weisberg M. K., Prinz M., Clayton R. N., Mayeda T. K., Grady M. M., Franchi I., Pillinger C. T. and Kallemeyn G. W. (1996) The K (Kakangari) chondrite grouplet. *Geochim. Cosmochim. Acta* **60**, 4253–4263.

Welten K. C., Nishiizumi K., Masarik J., Caffee M. W., Jull A. J. T., Klandrud S. E. And Wieler R. (2000) Cosmic-ray exposure history of two Frontier Mountain H-chondrite showers from spallation and neutron-capture products. *Meteorit. Planet. Sci*. **36**, 301-317.

Whillans I. M. and Cassidy W. A. (1983) Catch a falling star: Meteorites and old ice. *Science* **222**, 55-57.

de Winter N. J. and Claeys Ph. (2017) Micro X-ray fluorescence (µXRF) line scanning on Cretaceous rudist bivalves: A new method for reproducible trace element profiles in bivalve calcite. *Sedimentology* **64**, 231-251.

Yamaguchi A., Shiraishi K. and Harvey R. (2021) The discovery of meteorites near the Yamato Mountains: How the 1969 discoveries changed planetary science. *Meteorit. Planet. Sci*. **56**, 11-12.

Zanda B., Bourot-Denise M., Perron C. and Hewins R. H. (1994) Origin and metamorphic redistribution of silicon, chromium and phosphorus in the metal of chondrites. *Science* **265**, 1846–1849.

TABLE CAPTIONS

Table 1. List of H chondrites analyzed in this study.

* The shock stages are estimated from descriptions of the shock degree in Meteorite Newsletter, NIPR, based on Stöffler *et al*. (1991).

[a] Meteorite Newsletter, NIPR. [b] Antarctic Meteorite Newsletter, NASA.

Meteorite	Section Number		Type[a, b]	Weathering[a, b] index	Shock stage	Sources
	PTS	Powder				
A-881258	71-A	82	H3.0	B	?	NIPR
A-880941	51-A	48	H3.3	A/B	S1-2*	NIPR
Y-793574	51-A	56	H3.5	?	?	NIPR
Y-790461	91-A	100	H3.7	B	S3*	NIPR
ALH 78084	81-A	89	H3.9	B/Ce	?	NIPR
A 09436	-	-	H3	C	?	RBINS
A 09387	-	-	H4	B/C	?	RBINS
A 09618	-	-	H5	C	?	RBINS
A 09516	-	-	H6	C	?	RBINS
Y-790960	63-A	62	H7	B	S3*	NIPR
NWA 6752	-	-	H3	W2	S1	RBINS
NWA 6771	-	-	H4	W1	S1	RBINS
Sahara 97035	-	-	H5	W2	S1	RBINS

Table 2. Elemental abundances and isotope compositions in BHVO-2 (ID: isotope dilution, n.a.: not analyzed).

The uncertainties of elemental abundances (1SD), ^{143}Nd/^{144}Nd, and ^{176}Hf/^{177}Hf (2SE) reflect internal reproducibilities during the measurements by ICP-OES, Q-ICP-MS, and MC-ICP-MS. The uncertainties of the elemental abundances (ID), ^{147}Sm/^{144}Nd, and ^{176}Lu/^{177}Hf (2SE) reflect the maximum uncertainties due to spike calibrations (see subsection 2.3.2).

* The uncertainty of the ^{176}Hf/^{177}Hf value (2SE) reflects external reproducibilities during the measurements of MC-ICP-MS.

[a] Jochum *et al*. (2016) for elemental abundances including those determined by isotope dilution, ^{147}Sm/^{144}Nd, and ^{176}Lu/^{177}Hf. [b] Weis *et al*. (2006) for ^{143}Nd/^{144}Nd. [c] Weis *et al*. (2007) for ^{176}Hf/^{177}Hf.

	This work		Preferred values[a-c]
(%)			
Na	1.79 ± 0.00	1.59 ± 0.02	1.646 ± 0.036
Mg	4.74 ± 0.03	4.44 ± 0.02	4.376 ± 0.025
Al	7.79 ± 0.05	6.87 ± 0.03	7.113 ± 0.032
P	0.115 ± 0.002	0.114 ± 0.003	0.1172 ± 0.0022
K	0.439 ± 0.005	0.416 ± 0.001	0.4259 ± 0.0031
Ca	8.15 ± 0.02	7.66 ± 0.03	8.148 ± 0.043
Ti	1.68 ± 0.01	1.57 ± 0.00	1.637 ± 0.011
Cr	0.0310 ± 0.0008	0.0335 ± 0.0004	0.02872 ± 0.00031
Mn	0.129 ± 0.002	0.130 ± 0.002	0.1309 ± 0.0015
Fe	8.73 ± 0.01	8.30 ± 0.01	8.666 ± 0.063
(ppm)			
Ni	127 ± 31	127 ± 4	119.8 ± 1.2
Co	80.8 ± 1.7	76.5 ± 1.9	44.89 ± 0.32
Cu	123 ± 1	119 ± 1	129.3 ± 1.4
Zn	97.9 ± 0.5	123 ± 1	103.9 ± 1.0
Rb	9.91 ± 0.10	8.24 ± 0.19	9.261 ± 0.096
Sr	370 ± 2	354 ± 5	394.1 ± 1.7
Y	25.7 ± 0.1	24.3 ± 0.2	25.91 ± 0.28
Zr	165 ± 1	157 ± 1	171.2 ± 1.3
Nb	16.9 ± 0.1	16.4 ± 0.1	18.10 ± 0.20
Ba	126 ± 1	121 ± 2	130.9 ± 1.0
La	15.7 ± 0.2	15.2 ± 0.2	15.20 ± 0.08
Ce	37.7 ± 0.4	36.5 ± 0.5	37.53 ± 0.19
Pr	5.20 ± 0.03	5.08 ± 0.08	5.339 ± 0.028
Nd	24.7 ± 0.2	23.7 ± 0.4	24.27 ± 0.25
Sm	6.01 ± 0.13	5.75 ± 0.1	6.023 ± 0.057
Eu	2.02 ± 0.03	1.98 ± 0.03	2.043 ± 0.012
Gd	6.47 ± 0.11	6.18 ± 0.12	6.207 ± 0.038
Tb	0.914 ± 0.012	0.876 ± 0.020	0.9392 ± 0.0053
Dy	5.29 ± 0.05	5.11 ± 0.08	5.280 ± 0.028
Ho	0.980 ± 0.015	0.940 ± 0.020	0.9887 ± 0.0053
Er	2.57 ± 0.03	2.43 ± 0.04	2.511 ± 0.014
Tm	0.335 ± 0.004	0.315 ± 0.012	0.3349 ± 0.0031
Yb	2.00 ± 0.06	1.93 ± 0.01	1.994 ± 0.027
Lu	0.278 ± 0.005	0.256 ± 0.008	0.2754 ± 0.0024
Hf	4.40 ± 0.04	4.06 ± 0.12	4.470 ± 0.025
Th	1.38 ± 0.06	1.14 ± 0.05	1.224 ± 0.016
U	0.412 ± 0.007	0.377 ± 0.012	0.412 ± 0.035
Nd (ID)	n.a.	22.5 ± 0.1	24.27 ± 0.18
Sm (ID)		5.63 ± 0.03	6.023 ± 0.038
Lu (ID)		0.249 ± 0.001	0.2754 ± 0.0018
Hf (ID)		4.04 ± 0.02	4.470 ± 0.020

Table 3. Modal abundances in H chondrites: vol. % at left; wt. % at right (UHC: unequilibrated H chondrite, EHC: equilibrated H chondrite). Wt. % is calculated from vol. % using the following estimated mineral specific gravities and normalized to 100%: olivine (3.48), low-Ca pyroxene (3.2). Ca-pyroxene (3.4), feldspar (2.62), kamacite (7.9), taenite (8.01), troilite (4.61), chlorapatite (3.16), merrillite (3.12), chromite (4.6).

The uncertainties for the mean values from this study are 95% confidence interval, and those for McSween *et al*., (1991) are 2SE calculated from their data.

* The modal abundances of low-Ca pyroxene, feldspar, and chromite obtained in this study may include forsterite, silica, and ilmenite, respectively (see section 3.1).

Name	A-881258		A-880941		Y-793574		Y-790461		ALH 78084		A 09436		A 09387		A 09618		A 09516		Y-790960	
Area (mm^2)	71.294		52.706		61.594		104.907		81.524		190.921		89.756		152.775		177.284		34.607	
Olivine	40.7	38.9	36.8	33.4	34.4	32.2	38.0	35.9	35.8	33.5	35.4	33.1	36.8	35.4	38.0	35.6	36.8	33.4	38.7	36.0
Low-Ca pyroxene*	30.7	27	24.1	20	27.4	24	26.8	23	29.7	26	32.8	28	29.2	26	30.6	26	30.8	26	29.0	25
Ca-pyroxene	1.15	1.1	6.26	5.6	7.88	7.2	5.53	5.1	5.51	5.0	4.52	4.1	4.86	4.6	2.26	2.1	3.94	3.5	5.02	4.6
Feldspar*	14.8	10.7	14.5	9.91	14.6	10.3	14.7	10.5	14.1	9.91	13.1	9.22	14.3	10.3	13.6	9.58	10.9	7.45	14.0	9.77
Kamacite	6.01	13	3.52	7.2	5.76	12	6.05	13	6.64	14	6.09	13	4.81	10	7.23	15	7.35	15	6.46	14
Taenite	1.59	3.49	8.85	18.5	3.49	7.51	2.67	5.82	2.86	6.17	3.15	6.76	2.91	6.44	2.06	4.45	4.40	9.19	2.59	5.54
Troilite	3.59	4.55	3.12	3.75	4.33	5.36	3.93	4.92	3.47	4.30	3.74	4.62	4.04	5.15	3.97	4.94	3.50	4.20	3.79	4.67
Chlorapatite	0.05	0.04	0.09	0.07	0.11	0.10	0.05	0.04	0.29	0.25	0.16	0.14	0.03	0.02	0.30	0.26	0.14	0.11	0.35	0.30
Merrillite	0.47	0.41	0.37	0.30	0.38	0.32	0.41	0.35	0.32	0.27	0.36	0.30	0.90	0.78	0.33	0.28	0.78	0.64	0.43	0.36
Total Ca-phosphates	0.52	0.45	0.46	0.38	0.49	0.41	0.46	0.39	0.61	0.51	0.52	0.44	0.93	0.80	0.63	0.53	0.92	0.75	0.78	0.66
Chromite*	0.59	0.74	0.97	1.2	1.05	1.3	0.81	1.0	0.72	0.89	0.60	0.74	0.77	0.97	0.79	0.98	0.63	0.76	0.28	0.35
Iron oxide	-		trace		trace		-		trace		trace		-		-		-		-	
Silica	-		-		-		trace		-		-		trace		-		-		-	
(Mg, Fe)-spinel	-		trace		-		trace		-		-		-		-		-		-	
Hibonite	-		-		-		trace		-		-		-		-		-		-	
(Zn, Fe)S	-		-		-		-		-		trace		trace		-		-		-	

Total	99.6	98.6	99.3	99.0	99.3	100.0	98.6	99.0	99.3	100.7

(*continued*)

Name	NWA 6752		NWA 6771		Sahara 97035		UHC mean (this study)		EHC mean (this study)		EHC mean (literature data; in wt. %)	
Area (mm^2)/ n / Ref.	496.441		94.315		100.041		n = 7		n = 6		Van Schmus (1969)	McSween *et al.* (1991), n = 25
Olivine	38.0	34.5	39.3	36.4	35.3	33.7	37.0 ± 1.9	34.5 ± 2.4	37.5 ± 1.5	35.1 ± 1.3	33 - 37	35.7 ± 1.5
Low-Ca pyroxene*	31.2	26	26.4	22	30.1	26	29.0 ± 2.8	25 ± 3	29.4 ± 1.7	25 ±2	23 - 27	26.3 ± 1.2
Ca-pyroxene	2.02	1.8	5.55	5.0	5.50	5.1	4.70 ± 2.19	4.3 ± 2.0	4.52 ± 1.31	4.1 ± 1.2	4 - 5	4.1 ± 0.2
Feldspar*	9.00	6.15	12.1	8.40	13.8	9.89	13.5 ± 1.9	9.52 ± 0.58	13.1 ± 1.4	9.24 ± 1.14	9 - 10	9.6 ± 0.2
Kamacite	7.30	15	7.21	15	6.88	15	5.91 ± 1.09	13 ± 3	6.65 ± 1.01	14 ± 2	15 - 17	18.2 ± 0.6
Taenite	4.54	9.48	2.88	6.13	1.51	3.32	3.88 ± 2.19	8.25 ± 4.64	2.72 ± 1.03	5.84 ± 2.10	2 - 3	
Troilite	4.88	5.86	3.95	4.85	4.06	5.14	3.86 ± 0.54	4.77 ± 0.47	3.89 ± 0.22	4.82 ± 0.37	5 - 6	5.5 ± 0.2
Chlorapatite	0.06	0.05	0.42	0.35	trace		0.12 ± 0.08	0.10 ± 0.07	0.21 ± 0.17	0.17 ± 0.14	-	-
Merrillite	0.14	0.12	0.41	0.34	0.89	0.76	0.35 ± 0.10	0.29 ± 0.08	0.62 ± 0.27	0.53 ± 0.24	-	-
Total Ca-phosphates	0.20	0.17	0.83	0.69	0.89	0.76	0.47 ± 0.12	0.39 ± 0.09	0.83 ± 0.12	0.70 ± 0.10	0.6	0.65 ± 0.03
Chromite*	0.83	0.99	0.80	0.98	0.48	0.60	0.79 ± 0.16	0.98 ± 0.20	0.63 ± 0.22	0.77 ± 0.27	0.5	0.76 ± 0.02
Iron oxide	trace		-		-							
Silica	-		-		-							
(Mg, Fe)-spinel	-		-		-							
Hibonite	-		-		-							
(Zn, Fe)S	-		-		-							
Total	98.0		98.9		98.5							

Table 4. Elemental abundances and isotope compositions in H chondrites (UHC: unequilibrated H chondrite, EHC: equilibrated H chondrite, ID: isotope dilution, n.d.: not determined).
The uncertainties for each sample reflect the same as those in Table 2 and the number of digits is based on the reproducibility of the reference material. The uncertainties for the mean values are 95% confidence interval. The elemental abundances (ID) and the isotope ratios for non-Antarctic HC are mean values of H chondrite falls from the following literatures (see Supplementary data).
* The data of A 09516 (H6) are excluded from the means (see section 3.2).
[a] Jarosewich (1990) for Na-Ni. [b] Wasson and Kallemeyn (1988) for Cu-Ba and Hf. [c] Nakamura (1974) for REEs. [d] Tatsumoto *et al.* (1973) for Th and U. [e] Jacobsen and Wasserburg (1980, 1984), Patchett *et al.* (2004), Boyet and Carlson (2005), Carlson *et al.* (2007), Bouvier *et al.* (2008), Gannoun *et al.* (2011), Burkhardt *et al.* (2016), and Fukai and Yokoyama (2017) for Nd and Sm isotope compositions. [f] Blichert-Toft and Albarède (1997), Bizzarro *et al.* (2003), Patchett *et al.* (2004), Bouvier *et al.* (2008), and Dauphas and Pourmand (2011) for Lu and Hf isotope compositions.

Name	A-881258	A-880941	Y-793574	Y-790461	ALH 78084
(%)					
Na	0.56 ± 0.03	0.54 ± 0.04	0.68 ± 0.04	0.61 ± 0.01	0.62 ± 0.03
Mg	14 ± 0	13 ± 0	15 ± 0	14 ± 0	14 ± 0
Al	0.99 ± 0.00	0.92 ± 0.00	1.1 ± 0.0	1.1 ± 0.0	1.0 ± 0.00
P	0.11 ± 0.00	0.11 ± 0.00	0.13 ± 0.00	0.12 ± 0.00	0.10 ± 0.00
K	0.065 ± 0.001	0.050 ± 0.001	0.071 ± 0.002	0.065 ± 0.002	0.065 ± 0.001
Ca	0.98 ± 0.00	0.94 ± 0.01	1.2 ± 0.0	1.0 ± 0.0	1.0 ± 0.0
Ti	0.057 ± 0.01	0.050 ± 0.002	0.061 ± 0.002	0.062 ± 0.001	0.055 ± 0.000
Cr	0.38 ± 0.00	0.34 ± 0.00	0.41 ± 0.00	0.40 ± 0.00	0.35 ± 0.00
Mn	0.23 ± 0.00	0.22 ± 0.00	0.25 ± 0.00	0.23 ± 0.00	0.23 ± 0.00
Fe	23 ± 1	22 ± 0	27 ± 0	23 ± 0	22 ± 0
Ni	1.6 ± 0.0	1.6 ± 0.0	1.6 ± 0.1	1.5 ± 0	1.5 ± 0.0
Co	0.064 ± 0.001	0.066 ± 0.000	0.085 ± 0.001	0.060 ± 0.000	0.065 ± 0.01
(ppm)					
Cu	88.0 ± 0.6	80.0 ± 1.6	78.0 ± 1.4	90.5 ± 1.8	75.2 ± 1.7
Zn	63.9 ± 0.8	52.1 ± 1.3	61.4 ± 0.9	61.2 ± 0.7	54.8 ± 1.3
Rb	2.45 ± 0.08	1.29 ± 0.05	2.29 ± 0.05	2.67 ± 0.07	2.26 ± 0.08
Sr	8.77 ± 0.13	8.76 ± 0.14	8.53 ± 0.14	9.42 ± 0.12	8.66 ± 0.23
Y	1.90 ± 0.02	1.97 ± 0.06	1.87 ± 0.04	1.98 ± 0.05	2.08 ± 0.05
Zr	4.78 ± 0.08	4.79 ± 0.10	4.69 ± 0.08	5.28 ± 0.09	5.31 ± 0.02
Nb	0.358 ± 0.014	0.356 ± 0.008	0.375 ± 0.007	0.370 ± 0.015	0.382 ± 0.008
Ba	3.19 ± 0.07	3.17 ± 0.07	3.06 ± 0.01	3.38 ± 0.02	3.18 ± 0.02

(ppb)					
La	299 ± 10	330 ± 8	324 ± 4	333 ± 10	317 ± 15
Ce	788 ± 19	833 ± 24	830 ± 21	850 ± 22	820 ± 40
Pr	116 ± 4	121 ± 8	119 ± 2	125 ± 4	113 ± 2
Nd	549 ± 19	602 ± 53	618 ± 14	581 ± 42	615 ± 60
Sm	177 ± 15	216 ± 12	181 ± 6	208 ± 12	188 ± 18
Eu	72.9 ± 3.4	73.8 ± 4.8	74.3 ± 3.0	76.6 ± 5.4	65.3 ± 4.8
Gd	257 ± 15	283 ± 17	292 ± 8	289 ± 19	285 ± 17
Tb	45.1 ± 2.7	47.2 ± 3.2	49.8 ± 0.9	46.9 ± 2.6	47.5 ± 2.5
Dy	324 ± 8	335 ± 11	337 ± 17	338 ± 20	365 ± 15
Ho	67.5 ± 3.0	75.0 ± 2.7	75.8 ± 1.5	74.3 ± 2.6	77.6 ± 2.3
Er	206 ± 3	215 ± 9	226 ± 7	232 ± 3	229 ± 4
Tm	30.2 ± 0.7	32.1 ± 1.7	34.6 ± 2.0	32.3 ± 1.4	31.5 ± 1.6
Yb	210 ± 12	210 ± 5	226 ± 8	211 ± 13	220 ± 9
Lu	30.1 ± 3.1	31.7 ± 4.3	34.3 ± 2.1	32.8 ± 2.7	30.0 ± 0.6
Hf	123 ± 9	135 ± 3	140 ± 10	147 ± 14	149 ± 7
Th	42.7 ± 1.4	38.1 ± 0.9	42.4 ± 0.6	43.0 ± 2.5	39.7 ± 1.9
U	11.4 ± 1.1	9.99 ± 0.64	12.4 ± 0.4	10.8 ± 0.5	12.0 ± 0.7
Nd (ID)	585 ± 3	609 ± 3	527 ± 3	604 ± 3	543 ± 3
Sm (ID)	190 ± 1	196 ± 1	172 ± 1	197 ± 1	178 ± 1
Lu (ID)	28.9 ± 0.1	29.7 ± 0.1	32.4 ± 0.2	29.2 ± 0.1	31.0 ± 0.2
Hf (ID)	123 ± 1	125 ± 1	152 ± 1	136 ± 1	140 ± 1
^{147}Sm/^{144}Nd	0.1958 ± 0.0014	0.1949 ± 0.0014	0.1977 ± 0.0014	0.1971 ± 0.0014	0.1986 ± 0.0014
^{143}Nd/^{144}Nd	0.512604 ± 0.000007	0.512570 ± 0.000014	0.512712 ± 0.000009	0.512585 ± 0.000008	0.512619 ± 0.000008
^{176}Lu/^{177}Hf	0.0336 ± 0.0002	0.0338 ± 0.0002	0.0304 ± 0.0002	0.0306 ± 0.0002	0.0315 ± 0.0002
^{176}Hf/^{177}Hf	0.282825 ± 0.000015	0.282868 ± 0.000016	0.282825 ± 0.000038	0.282689 ± 0.000019	0.282702 ± 0.000013

Table 5. Elemental abundance ratios in H chondrites (UHC: unequilibrated H chondrite, EHC: equilibrated H chondrite).

The uncertainties are derived from the uncertainties of the respective elemental abundances. The uncertainties for the mean values are 95% confidence interval. The mean values of non-Antarctic HC and Antarctic HC are calculated from the following literatures.

* The data of A 09516 (H6) are excluded from the means (see section 3.2).

[a] Jarosewich (1990) for Na and Al. [b] Wasson and Kallemeyn (1988) for Rb, Sr, and Ba. [c] Nishikawa *et al.*, (1990) for Rb, Sr, and Ba.

Name	$\frac{\mathrm{Rb}}{(\mathrm{Na}+\mathrm{Al})/2}$	$\frac{\mathrm{Sr}}{(\mathrm{Na}+\mathrm{Al})/2}$	$\frac{\mathrm{Ba}}{(\mathrm{Na}+\mathrm{Al})/2}$
A-881258	3.16 ± 0.12	11.3 ± 0.3	4.11 ± 0.14
A-880941	1.77 ± 0.09	12.0 ± 0.5	4.35 ± 0.18
Y-793574	2.56 ± 0.09	9.55 ± 0.32	3.43 ± 0.15
Y-790461	3.19 ± 0.09	11.3 ± 0.2	4.04 ± 0.24
ALH 78084	2.80 ± 0.13	10.7 ± 0.4	3.94 ± 0.24
A 09436-1	2.32 ± 0.05	10.7 ± 0.2	4.04 ± 0.15
A 09436-2	2.38 ± 0.07	11.1 ± 0.2	4.23 ± 0.11
A 09387	3.77 ± 0.11	10.7 ± 0.3	3.88 ± 0.11
A 09618	2.65 ± 0.06	11.0 ± 0.2	3.96 ± 0.08
A 09516-1	0.895 ± 0.049	8.71 ± 0.35	3.19 ± 0.15
A 09516-2	1.29 ± 0.07	12.3 ± 0.5	5.24 ± 0.31
Y-790960	3.11 ± 0.22	10.4 ± 0.3	3.65 ± 0.25
NWA 6752	2.51 ± 0.09	26.5 ± 0.7	202 ± 6
NWA 6771	3.21 ± 0.08	21.8 ± 0.5	22.9 ± 0.5
Sahara 97035	3.96 ± 0.13	123 ± 3	51.4 ± 1.3
Antarctic UHC mean (n = 7)	2.60 ± 0.50	11.0 ± 0.8	4.02 ± 0.29
Antarctic EHC mean* (n = 3)	3.17 ± 0.56	10.7 ± 0.3	3.83 ± 0.16
Antarctic HC mean* (n = 10)	2.77 ± 0.56	10.9 ± 0.7	3.96 ± 0.27
Hot desert HC mean (n = 3)	3.23 ± 3.23	57.2 ± 57.4	92.1 ± 96.3
Non-Antarctic HC mean[a, b]	3.28 ± 0.09	11.3 ± 0.3	4.74 ± 0.13
Antarctic HC mean[a, c]	3.24 ± 0.48	10.5 ± 1.1	3.04 ± 0.85

Table 6. Correlation coefficients (*r*) between elemental ratios and isotopic ratios in Antarctic HCs. Strong and no correlations are defined as |*r*| > 0.6 and 0.4 > |*r*|, and are shown in bolded and underlined, respectively.

	Correlation coefficients for all samples				Correlation coefficients excluding A 09516 (H6)			
	^{147}Sm/^{144}Nd	^{143}Nd/^{144}Nd	^{176}Lu/^{177}Hf	^{176}Hf/^{177}Hf	^{147}Sm/^{144}Nd	^{143}Nd/^{144}Nd	^{176}Lu/^{177}Hf	^{176}Hf/^{177}Hf
Al/Mg	-0.50	0.29	-0.42	-0.12	-0.21	-0.47	-0.36	-0.51
P/Mg	0.48	-0.57	**0.64**	**0.62**	**-0.60**	-0.45	-0.04	0.09
Ca/Mg	0.19	0.40	-0.24	-0.01	0.14	0.45	**-0.74**	-0.54
Ti/Mg	-0.42	0.28	**-0.63**	-0.43	-0.23	-0.01	**-0.79**	**-0.73**
Y/Mg	**0.65**	**-0.65**	**0.78**	**0.66**	0.04	-0.48	0.56	0.40
P/Ca	0.33	**-0.74**	**0.74**	**0.60**	-0.47	**-0.63**	0.58	0.50
Y/Ca	0.41	**-0.71**	**0.75**	0.49	-0.06	-0.55	**0.80**	0.58

Table 7. Major hosts of REEs and Hf, and alteration types for chondrites.

[a] Curtis and Schmitt (1979) and Ebihara and Honda (1983). [b] Larimer and Ganapathy (1987) and Ebihara (1988). [c] Martin *et al.* (2013). [d] Ebihara and Honda (1987). [e] Maeda *et al.* (2017a, 2017b). [f] Alexander (1994) and Mason and Graham (1970). [g] Barrat *et al.* (2014). [h] Krot *et al.* (2003) and Huss *et al.* (2006). [i] Weisberg *et al.* (1996) and Barosch *et al.* (2020).

Chondrite	Major hosts of REEs	Major hosts of Hf	Alteration type
H, L, LL	Ca-phosphates[a]	Ca-pyroxene (silicates)[f]	
EH, EL	Oldhamite (CaS)[b]	Sulfides and silicates[g]	Thermal metamorphism[h]
CK	Ca-phosphates and silicates[c]	Silicates[c]	
CV	Ca, Al-rich inclusions (CAIs)[d]	?	Aqueous alteration and
CO	?	?	weak thermal metamorphism[h]
CI, CM, CR, CH, CB	?	?	Aqueous alteration[h]
Rumuruti	Ca-phosphates[e]	?	Thermal metamorphism[h]
Kakangari	?	?	Aqueous alteration and weak thermal metamorphism[i]

FIGURE CAPTIONS

Fig. 1. The mean modal abundances (wt. %) in UHC and EHC obtained in this study (n = 7 and 6, respectively). The mean modal abundances of low-Ca pyroxene, feldspar, and chromite may include forsterite, silica, and ilmenite, respectively (see section 3.1). The uncertainties represent 95% confidence interval of the mean values.

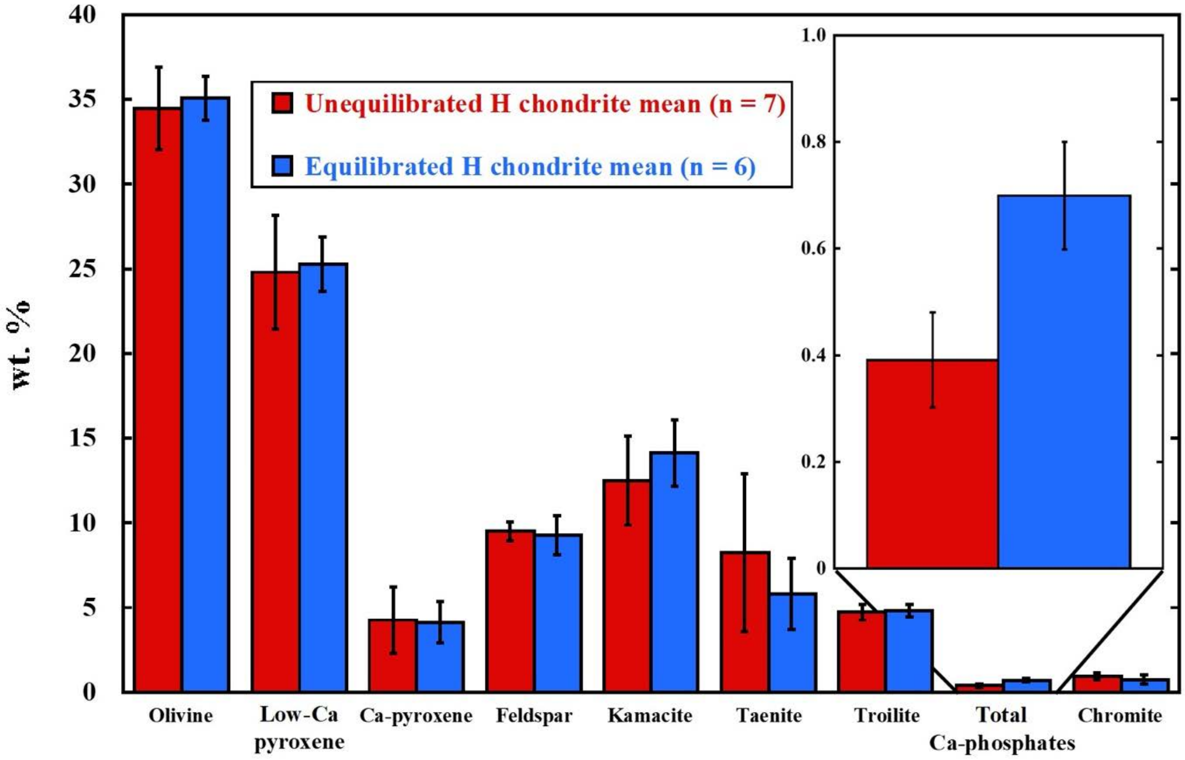

Fig. 2. CI-normalized REE, Th, and U abundances in each Antarctic and hot desert HC. The uncertainties represent 1SD of the measurements by Q-ICP-MS. Error bars are often smaller than the symbol size. Note that the scale of y-axis for hot desert is different from the other. CI values are from Anders and Grevesse (1989).

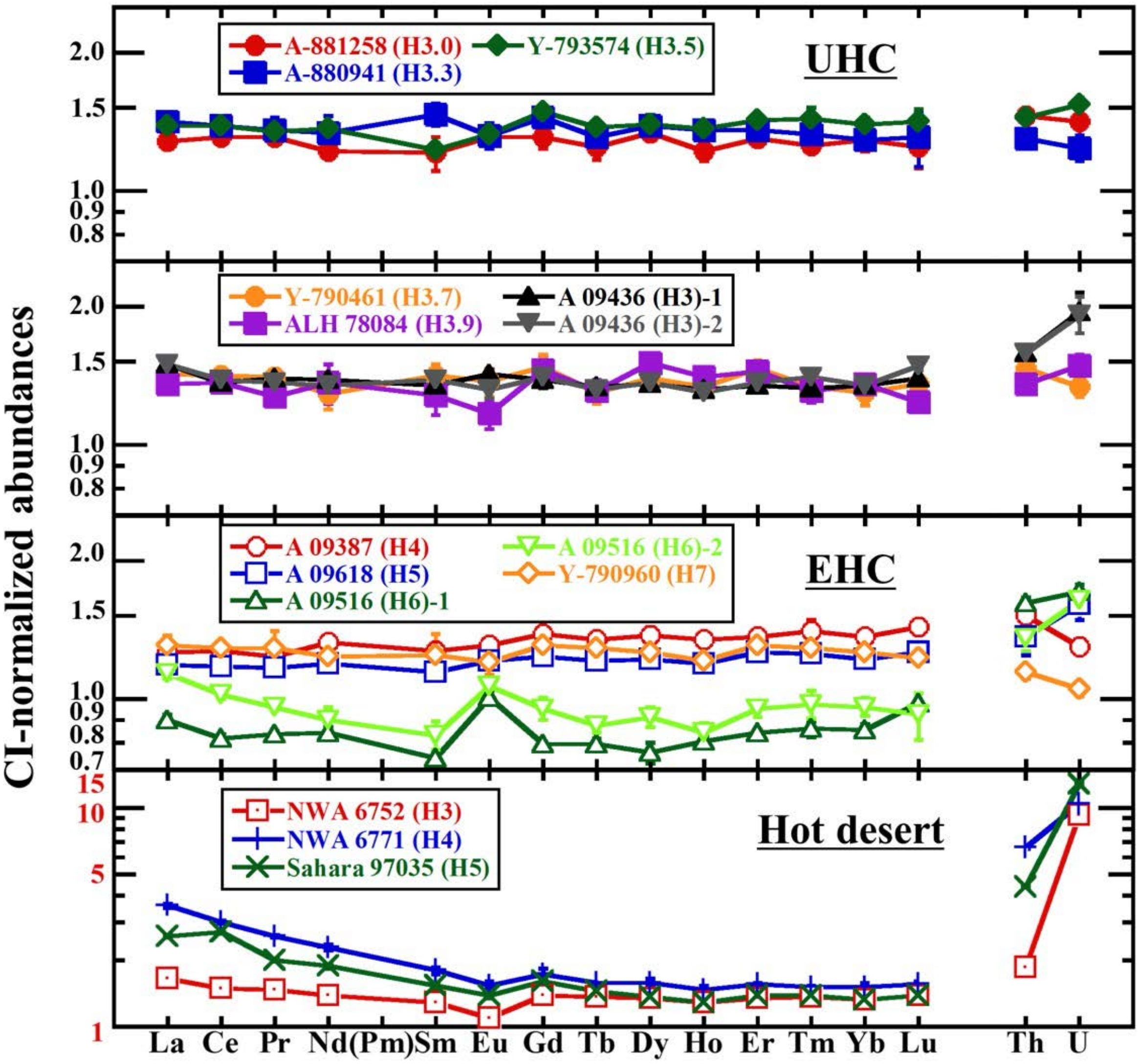

Fig. 3. Mean CI-normalized REE, Th, and U abundances of Antarctic UHCs, Antarctic EHCs, and Antarctic HCs (n = 7, 3, and 10, respectively). The mean values of non-Antarctic HCs are also shown for comparison (Nakamura, 1974 for REEs; Tatsumoto et al., 1973 for Th and U). The uncertainties are 95% confidence interval of the mean values. CI values from Anders and Grevesse (1989).

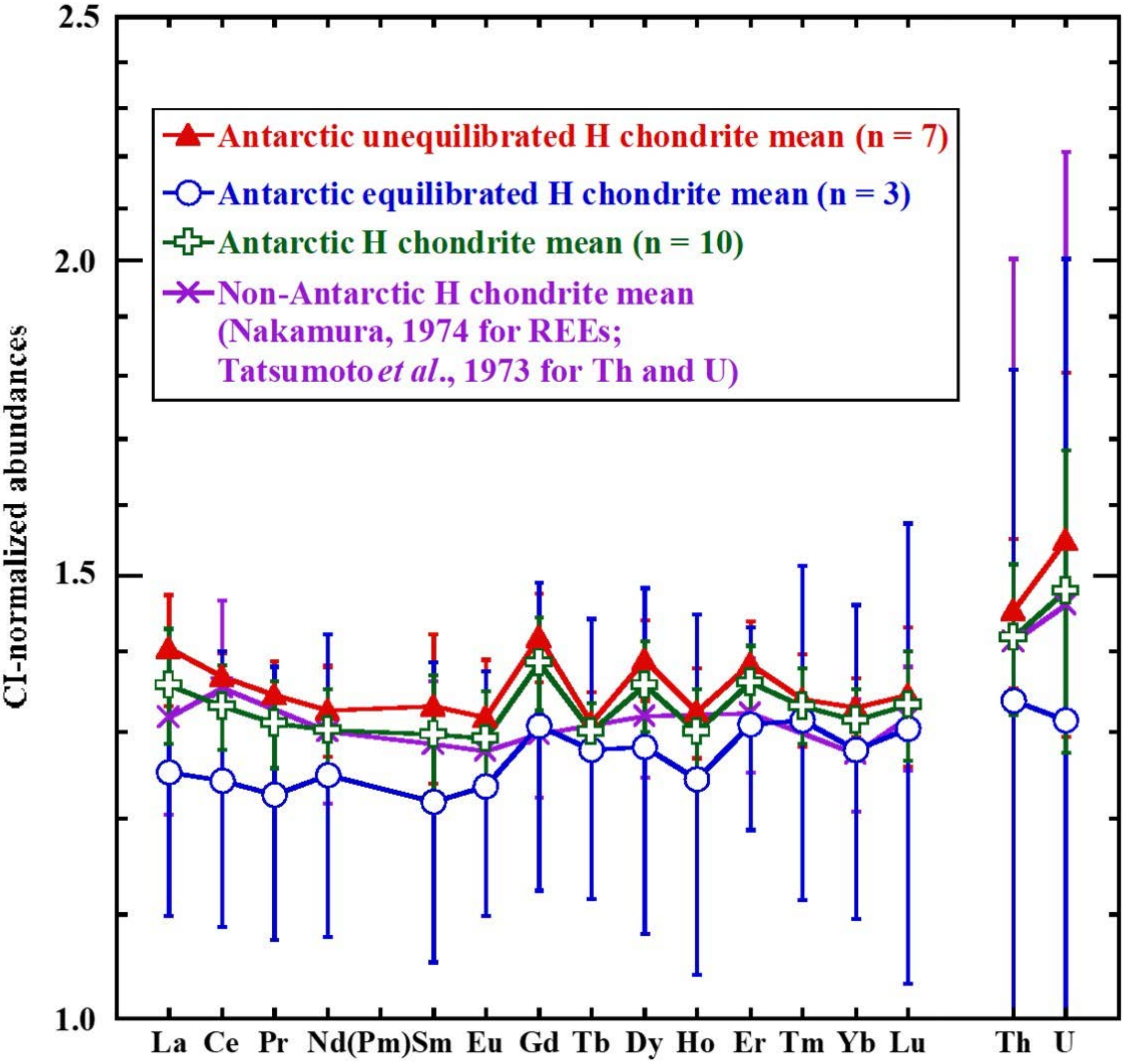

Fig. 4. Sm-Nd isotopic compositions of Antarctic UHCs, Antarctic EHCs, and HCs collected from hot deserts. The isotope compositions of chondrite falls, HC falls, and Antarctic chondrites from literatures are shown for comparison (Jacobsen and Wasserburg, 1980, 1984; Patchett *et al*., 2004; Boyet and Carlson, 2005; Carlson *et al*., 2007; Bouvier *et al*., 2008; Gannoun *et al*., 2011; Burkhardt *et al*., 2016; Fukai and Yokoyama, 2017; see Supplementary data for the details). The uncertainties for the ^{143}Nd/^{144}Nd values are 2SE of the internal reproducibility, and the uncertainties for the ^{147}Sm/^{144}Nd are 2SE of the total uncertainty derived from the uncertainty of the spike calibration (see subsection 2.3.2). Error bars are often smaller than the symbol size. The analytical uncertainties for the literature data are not shown. The chondrite isochron is from Bouvier *et al*. (2008).

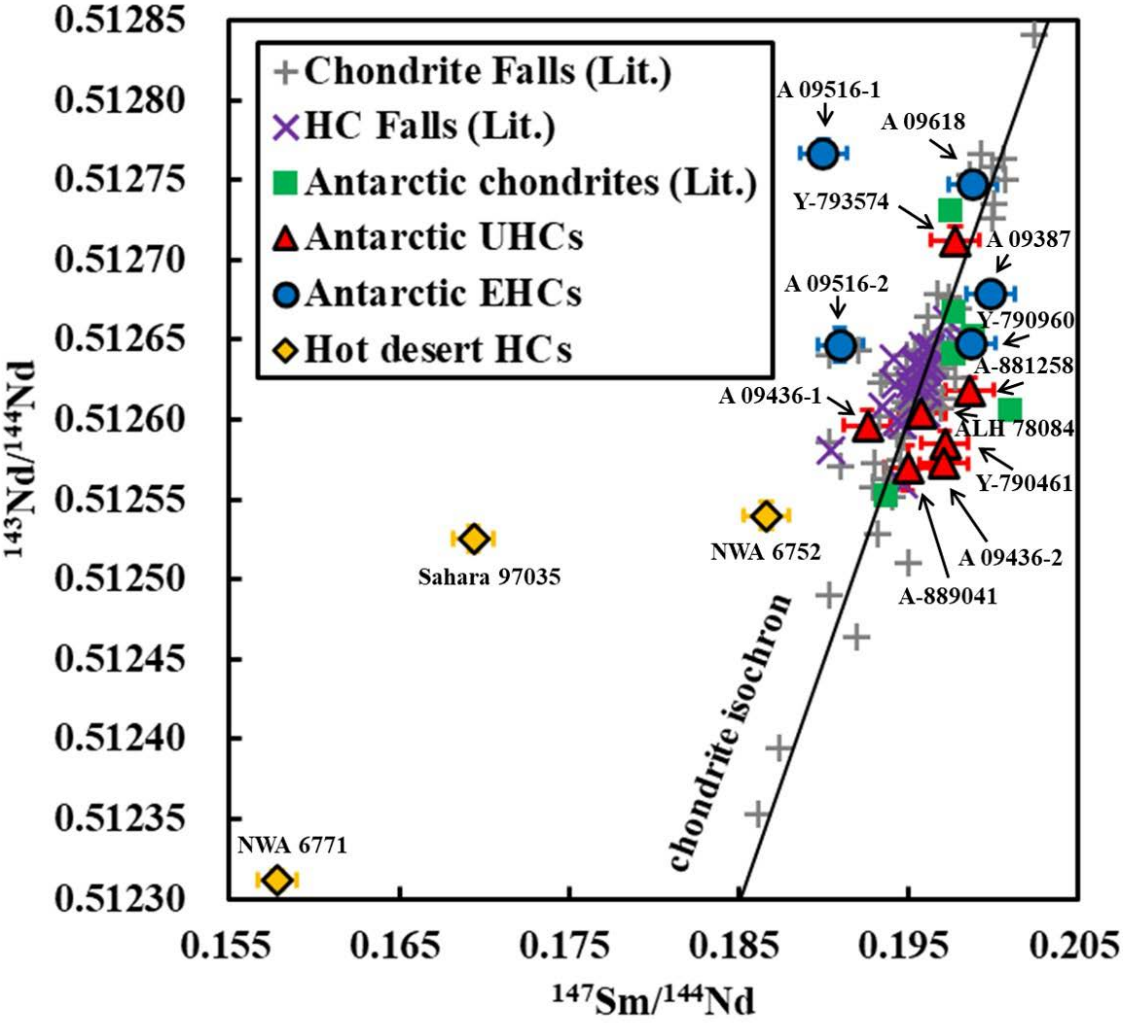

Fig. 5. Lu-Hf isotopic compositions of Antarctic UHCs, Antarctic EHCs, and HCs collected from hot deserts. The isotope compositions of chondrite falls, HC falls, and Antarctic chondrites from literature are also shown for comparison (Blichert-Toft and Albarède, 1997; Bizzarro *et al*., 2003; Patchett *et al*., 2004; Bouvier *et al*., 2008; Dauphas and Pourmand, 2011; see Supplementary data for the details). Note that Blichert-Toft and Albarède (1997) did not use high-pressure vessels during the sample digestion. The data of Farmington (L5), Adhi Kot (EH4), and Jajh Deh Kot Lalu (EL6) from Dauphas and Pourmand (2011) plot outside the range of the figure. The uncertainties for the $^{176}Hf/^{177}Hf$ values are 2SE of the internal reproducibility, and the uncertainties for the $^{176}Lu/^{177}Hf$ values are 2SE of the total uncertainty derived from the uncertainty of the spike calibration (see subsection 2.3.2). Error bars are often smaller than the symbol size. The analytical uncertainties for the literature data are not shown. The chondrite isochron is from Bouvier *et al*. (2008).

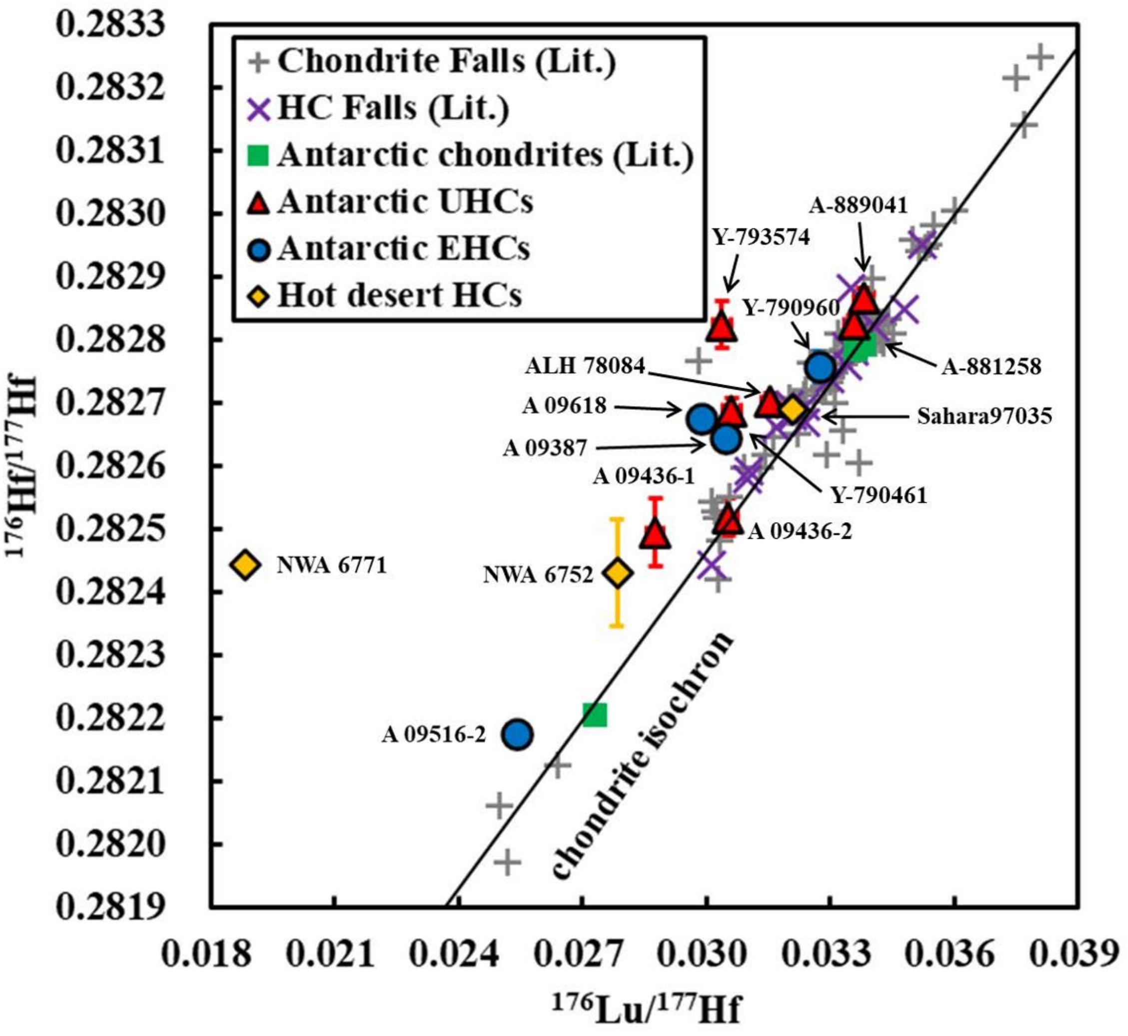

Fig. 6. Comparison of Rb and Sr abundances normalized by the mean Na and Al abundances, as a measure for the amount of feldspar in the sample. The plotted groups are divided based on their weathering index. The values for Non-Antarctic HC (Lit.) and Antarctic HC (Lit.) are calculated from Wasson and Kallemeyn (1988), Jarosewich (1990), and Nishikawa *et al*. (1990), shown in Table 5. The uncertainties are derived from the individual uncertainties of each elemental abundance, and those for literature values are 95% confidence interval of the mean values. Error bars are often smaller than the symbol size.

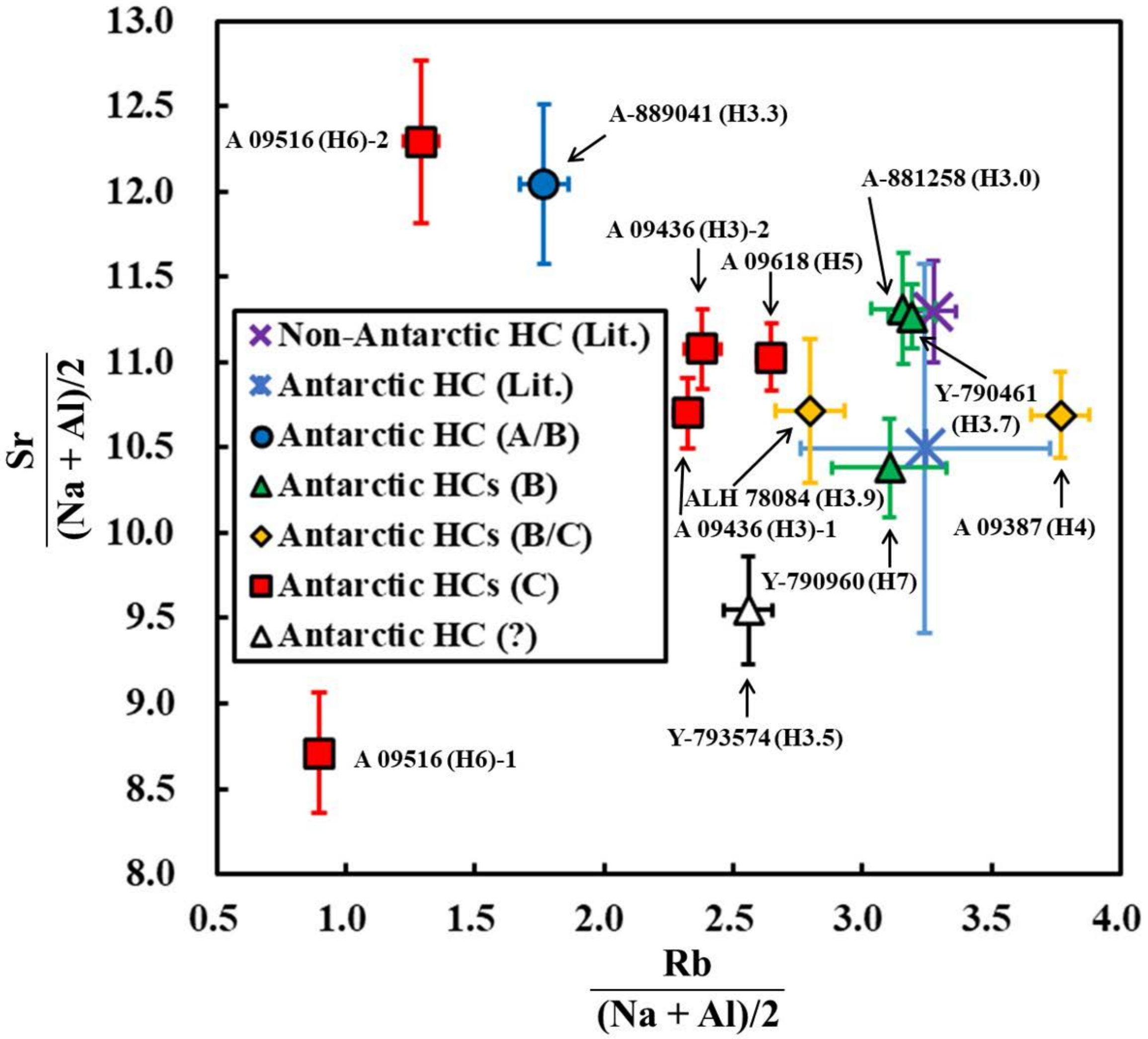

Fig. 7. Deviations of ^{147}Sm/^{144}Nd and ^{176}Lu/^{177}Hf from the respective chondrite isochron on Sm-Nd and Lu-Hf systems. The symbols of each plot reflect the weathering index and the Rb indicator (Table 5) by shape and color, respectively. Note that no weathering index for Y-793574 (H3.5) and ^{176}Hf/^{177}Hf of A 09516 (H6)-1 have been determined, hence the symbol of Y-793574 (H3.5) is not surrounded by black line and the δ^{176}Lu/^{177}Hf of A 09516 (H6)-1 was not determined. The ranges for chondrite falls and HC falls are calculated from the literature values shown in Figs. 4 and 5 (Supplemental data), and are shown by light green and light red, respectively. The respective isochrons used for the calculations are from Bouvier *et al.* (2008). The uncertainties except for the δ176Lu/177Hf of A 09516 (H6)-1 are derived from the uncertainties of each isotopic ratios. The uncertainties of the isochrons are not considered.

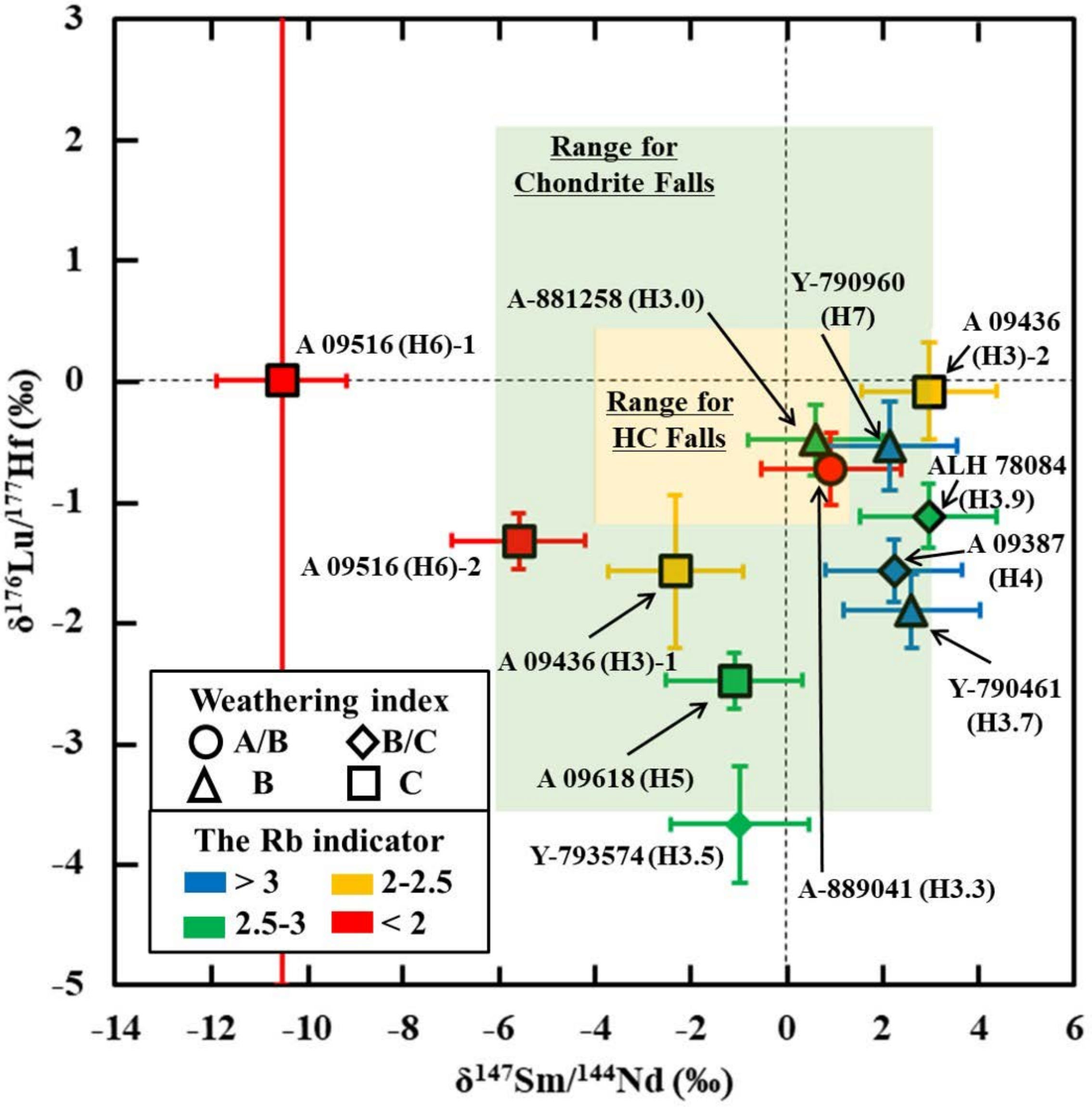

SUPPLEMENTARY DATA

Supplementary data-1. Sm-Nd and Lu-Hf isotopic compositions of H chondrite falls, chondrite falls, and Antarctic chondrites (WI: weathering index for Antarctic chondrites). The weathering indexes for Antarctic chondrites are from Antarctic Meteorite Newsletter, NASA. The chondrite fall mean includes H chondrites.
*MAC 88136 and MAC 88180 are possibly paired (Antarctic Meteorite Newsletter 13, NASA).
[a] Jacobsen and Wasserburg (1980. [b] Jacobsen and Wasserburg (1984). [c] Blichert-Toft and Albarède (1997). [d] Bizzarro *et al*. (2003). [e] Patchett *et al*. (2004). [f] Boyet and Carlson (2005). [g] Carlson *et al*. (2007). [h] Bouvier *et al*. (2008). [i] Dauphas and Pourmand (2011). [j] Gannoun *et al*. (2011). [k] Burkhardt *et al*. (2016). [l] Fukai and Yokoyama (2017).

Supplementary data-2. Average Sm-Nd and Lu-Hf isotope compositions in each class calculated using only falls from the supplementary data-1. The uncertainties associated with the isotopic ratios are simply calculated at 2SE, except for *N* = 2, where the values reflect the range of values. Tieschitz and Bjurböle are excluded from this calculation due to their intermediate petrologic features. The following samples are excluded from the respective means because their values seem not to be representative: Farmington from Dauphas and Purmand (2011), M'Bale from Bizzarro *et al*. (2003), and Peace River from Carlson *et al*. (2007) for the means of L chondrites; Paragould from Dauphas and Purmand (2011) and Saint-Séverin (Light) and (Dark) from Jacobsen and Wasserburg (1980) for the means of LL chondrites; Orgueil from Blichert-Toft and Albarède (1997) for the means of CI chondrites; the Sm-Nd values of Alende piece from Patchett et al. (2004) and Grosnaja from Carlson *et al*. (2007) for the means of CV chondrites; Abee and Abee (bis) from Burkhardt *et al*. (2016) and Adhi Kot, St. Mark's, and Saint-Sauveur from Dauphas and Purmand (2011) for the means of EH chondrites; Eagle, Jajh Deh Kot Lalu, and Khairpur from Dauphas and Purmand (2011) for the means of EL chondrites.

Sm-Nd and Lu-Hf isotope compositions of H chondrite falls, chondrite falls, and Antarctic chondrites (WI: weathering index for Antarctic chondrites).

Meteorite	Class	Nd (ppb)	Sm (ppb)	^{147}Sm/^{144}Nd	2SE	^{143}Nd/^{144}Nd	2SE	Lu (ppb)	Hf (ppb)	^{176}Lu/^{177}Hf	2SE	^{176}Hf/^{177}Hf	2SE	Ref.
<u>H chondrite Falls</u>														
Sharps	H3.4	572	186	0,1959	0,0002	0,512624	0,000006							f
Sharps (bis)	H3.4	592	190	0,1951	0,0002	0,512622	0,000002							f
Sharps	H3.4	570	185	0,1963	0,0010	0,512644	0,000009	33,6	143	0,0334	0,0002	0,282791	0,000007	h
Dhajala	H3.8	623	201	0,1954	0,0002	0,512621	0,000003							f
Dhajala	H3.8	576	186	0,1958	0,0010	0,512633	0,000008	33,2	143	0,0330	0,0002	0,282740	0,000006	h
Ankober	H4	541	175	0,1960	0,0004	0,512604	0,000006	30,7	137	0,0317	0,0002	0,282661	0,000008	e
Avanhandava	H4	562	182	0,1961	0,0004	0,512617	0,000005	32,8	144	0,0324	0,0002	0,282669	0,000018	e
Bielokrynitschie	H4							31,4	144	0,0310	0,0004	0,282581	0,000036	i
Ochansk	H4	491	158	0,1941	0,0004	0,512638	0,000006	31,6	149	0,0301	0,0002	0,282444	0,000009	e
Ochansk (bis)	H4	618	200	0,1960	0,0004	0,512630	0,000009	35,3	150	0,0334	0,0002	0,282761	0,000016	e
Ochansk	H4							34,0	151	0,0320	0,0004	0,282699	0,000036	i

Kesen	H4							32,4	133	0,0348	0,0004	0,282849	0,000036	i
Sainte Marguerite	H4	702	227	0,1955	0,0002	0,512635	0,000006							k
Sainte Marguerite (bis)	H4	773	250	0,1954	0,0002	0,512636	0,000005							k
Allegan	H5	570	185	0,1958	0,0004	0,512646	0,000010	32,1	129	0,0352	0,0002	0,282951	0,000014	e
Allegan	H5	584	188	0,1952	0,0002	0,512615	0,000003							k
Forest City	H5	624	203	0,1964	0,0004	0,512634	0,000006	35,8	151	0,0336	0,0002	0,282782	0,000012	e
Forest City	H5	675	217	0,1944	0,0002	0,512599	0,000003							k
Forest City	H5			0,1960	0,0030	0,512633	0,000003							l
Gao	H5							33,2	141	0,0335	0,0003	0,282884	0,000020	c
Herredia	H5							32,4	143	0,0321	0,0003	0,282681	0,000037	c
Herredia	H5							34,3	143	0,0341	0,0001	0,282821	0,000022	d
Jilin	H5	550	173	0,1904		0,512581	0,000003							j
Pultusk	H5	592	193	0,1973	0,0004	0,512663	0,000006	35,1	148	0,0337	0,0002	0,282810	0,000014	e
Pultusk	H5	660	211	0,1934	0,0002	0,512608	0,000005							k
Richardton	H5	562	184	0,1979	0,0004	0,512648	0,000006	33,3	153	0,0310	0,0002	0,282593	0,000009	e
Richardton	H5	595	191	0,1942	0,0002	0,512622	0,000003							f
Guareña	H6	902	290	0,1947	0,0002	0,512560	0,000024							a
Kernouve	H6							29,3	129	0,0324	0,0004	0,282695	0,000036	i
Queens Mercy	H6	587	189	0,1946	0,0002	0,512597	0,000003							k
Ucera	H	569	185	0,1963		0,512645	0,000001							g
HC fall mean		**613**	**198**	**0,1953**	**0,0006**	**0,512623**	**0,000009**	**33,0**	**143**	**0,0328**	**0,0007**	**0,282730**	**0,000060**	
***N* for the mean values**			***23***			***24***			***17***			***17***		
Chondrite Falls														
Tieschitz	H/L3.4	633	203	0,1937	0,0010	0,512628	0,000007	36,0	157	0,0325	0,0002	0,282766	0,000006	h
Hallingeberg	L3.4	616	200	0,1960	0,0010	0,512629	0,000007	35,1	148	0,0336	0,0002	0,282781	0,000007	h
Hedjaz	L3.7							32,6	141	0,0329	0,0001	0,282726	0,000021	d
Mezo-Madaras	L3.7	621	201	0,1960	0,0010	0,512626	0,000009	35,6	152	0,0333	0,0002	0,282764	0,000004	h
Bovedy	L3.8	687	223	0,1961	0,0010	0,512629	0,000007	40,3	172	0,0333	0,0002	0,282657	0,000009	h

Bald Mountain	L4							37,1	147	0,0360	0,0004	0,283005	0,000036	i
Saratov	L4			0,1960	0,0002	0,512616	0,000005							l
Tennasilm	L4							36,6	154	0,0337	0,0003	0,282606	0,000025	c
Tennasilm	L4							33,8	146	0,0329	0,0001	0,282720	0,000025	d
Farmington	L5							44,2	148	0,0425	0,0004	0,283741	0,000036	i
Farmington	L5	655	210	0,1944	0,0002	0,512591	0,000006							k
Homestead	L5	678	218	0,1949	0,0004	0,512640	0,000008	35,2	150	0,0332	0,0002	0,282810	0,000009	e
Homestead	L5	583	188	0,1951		0,512625	0,000001							g
Alfianello	L6							33,5	155	0,0317		0,282599	0,000014	c
Alfianello	L6							42,3	169	0,0355	0,0001	0,282982	0,000013	d
Bruderheim	L6	530	173	0,1970	0,0004	0,512648	0,000006	31,0	145	0,0302	0,0002	0,282518	0,000022	e
Bruderheim	L6	540	175	0,1955	0,0004	0,512620	0,000003							f
Bruderheim	L6	909	291	0,1935	0,0002	0,512563	0,000003							k
Fisher	L6							37,1	150	0,0350	0,0004	0,282959	0,000008	c
Girgenti	L6	674	218	0,1954	0,0004	0,512643	0,000006	38,2	173	0,0313	0,0002	0,282597	0,000009	e
Harleton	L6							32,0	150	0,0303	0,0004	0,282421	0,000036	i
Holbrook	L6	557	182	0,1975	0,0004	0,512656	0,000008	33,9	159	0,0303	0,0002	0,282483	0,000012	e
Holbrook (bis)	L6	571	187	0,1974	0,0004	0,512677	0,000009	34,0	160	0,0301	0,0002	0,282544	0,000014	e
Leedey	L6			0,1966	0,0004	0,512629	0,000023							b
M'Bale	L6							35,4	152	0,0331	0,0003	0,282700	0,000016	c
M'Bale	L6							30,2	162	0,0264	0,0001	0,282127	0,000011	d
M'Bale (bis)	L6							36,8	171	0,0306	0,0001	0,282552	0,000025	d
Modoc (1905)	L6			0,1950	0,0020	0,512510	0,000005							l
Peace River	L6	606	82	0,1903		0,512641	0,000001							g
Bjurböle	L/LL4	650	208	0,1933	0,0004	0,512602	0,000007	38,9	170	0,0324	0,0002	0,282714	0,000008	e
Semarkona	LL3.0	662	215	0,1960	0,0010	0,512622	0,000012	37,8	162	0,0331	0,0002	0,282749	0,000005	h
Krymka	LL3.1	601	193	0,1945	0,0010	0,512575	0,000012	34,2	144	0,0337	0,0002	0,282786	0,000008	h
Chainpur	LL3.5	633	205	0,1956	0,0010	0,512623	0,000008	36,1	154	0,0333	0,0002	0,282786	0,000005	h
Parnallee	LL3.6	648	210	0,1961	0,0010	0,512622	0,000010	37,1	156	0,0339	0,0002	0,282809	0,000005	h

Hamlet	LL4							39,0	177	0,0314	0,0004	0,282619	0,000036	i
Soko-Banja	LL4							33,8	149	0,0324	0,0004	0,282722	0,000036	i
Chelyabinsk	LL5	661	215	0,1963	0,0002	0,512647	0,000003							k
Tuxtuac	LL5							38,9	168	0,0329	0,0004	0,282619	0,000036	i
Tuxtuac	LL5			0,1920	0,0020	0,512643	0,000005							l
Paragould	LL5							45,2	172	0,0375	0,0004	0,283217	0,000036	i
Dhurmsala	LL6	593	193	0,1965	0,0002	0,512637	0,000003							k
Saint-Séverin (Light)	LL6	1386	440	0,1920	0,0002	0,512464	0,000025							a
Saint-Séverin (Dark)	LL6	560	185	0,2000	0,0002	0,512735	0,000027							a
Saint-Séverin (WR)	LL6			0,1964	0,0002	0,512618	0,000020							b
Saint-Séverin	LL6							42,7	185	0,0330	0,0004	0,282735	0,000036	i
Saint-Séverin	LL6			0,1910	0,0020	0,512571	0,000007							l
Ivuna	CI1	410	133	0,1967	0,0010	0,512679	0,000013							h
Ivuna	CI1							28,0	116	0,0343	0,0004	0,282826	0,000036	i
Orgueil	CI1							27,4	130	0,0298	0,0003	0,282767	0,000033	c
Orgueil	CI1	462	150	0,1968		0,512639	0,000001							g
Orgueil	CI1	459	149	0,1964	0,0010	0,512609	0,000014	25,1	106	0,0335	0,0002	0,282784	0,000005	h
Cold Bokkeveld	CM2	602	195	0,1962		0,512639	0,000001							g
Mighei	CM2	612	199	0,1966	0,0004	0,512644	0,000006	35,0	147	0,0339	0,0002	0,282798	0,000007	e
Mighei	CM2	625	202	0,1953		0,512618	0,000001							g
Mighei	CM2							33,0	139	0,0338	0,0004	0,282795	0,000036	i
Murchison	CM2	635	207	0,1969	0,0002	0,512607	0,000025							a
Murchison (bis)	CM2	670	214	0,1932	0,0002	0,512529	0,000034							a
Murchison (ter)	CM2	643	209	0,1966	0,0002	0,512628	0,000025							a
Murchison	CM2			0,1966	0,0002	0,512627	0,000016							b
Murchison	CM2							30,8	129	0,0340	0,0003	0,282899	0,000035	c
Murchison	CM2							34,0	150	0,0323	0,0001	0,282679	0,000019	d
Murchison	CM2	632	207	0,1977	0,0004	0,512626	0,000008	35,6	150	0,0338	0,0002	0,282804	0,000010	e
Murchison	CM2			0,1970	0,0020	0,512613	0,000005							l

Murray	CM2	641	207	0,1949	0,0004	0,512632	0,000007	36,1	155	0,0330	0,0002	0,282742	0,000011	e
Murray	CM2	638	207	0,1962		0,512637	0,000001							g
Pollen	CM2			0,1967	0,0002	0,512641	0,000024							b
Al Rais	CR2	548	179	0,1970	0,0010	0,512647	0,000009							h
Felix	CO3.1	735	238	0,1959	0,0010	0,512620	0,000007	46,3	196	0,0335	0,0002	0,282777	0,000004	h
Kainsaz	CO3.2	727	237	0,1969	0,0004	0,512632	0,000006	59,9	242	0,0351	0,0002	0,282942	0,000006	e
Kainsaz	CO3.2							43,8	186	0,0335	0,0004	0,282817	0,000036	i
Lancé	CO3.5	733	239	0,1969	0,0010	0,512647	0,000014	40,5	169	0,0339	0,0002	0,282799	0,000004	h
Lancé	CO3.5							42,5	177	0,0333	0,0004	0,282762	0,000036	i
Bali	CV3.6	771	256	0,2006	0,0010	0,512763	0,000014	40,6	171	0,0338	0,0002	0,282838	0,000009	h
Allende	CV3.6	1020	327	0,1940	0,0010	0,512552	0,000006	45,6	191	0,0339	0,0002	0,282816	0,000018	h
Allende (bis)	CV3.6	1021	327	0,1939	0,0010	0,512559	0,000010	45,7	190	0,0340	0,0002	0,282824	0,000005	h
Allende	CV3							49,8	211	0,0335	0,0003	0,282776	0,000015	c
Allende (bis)	CV3							46,1	192	0,0341	0,0003	0,282825	0,000011	c
Allende	CV3							43,3	186	0,0331	0,0001	0,282783	0,000012	d
Alende piece	CV3	1319	406	0,1861	0,0004	0,512353	0,000007	42,4	177	0,0341	0,0002	0,282847	0,000007	e
Allende pdr	CV3	1010	325	0,1947	0,0004	0,512606	0,000009	49,6	206	0,0341	0,0002	0,282828	0,000017	e
Allende pdr (bis)	CV3	991	319	0,1947	0,0004	0,512589	0,000009	48,1	198	0,0344	0,0002	0,282834	0,000016	e
Allende	CV3	986	315	0,1930	0,0002	0,512573	0,000003							f
Allende (bis)	CV3	1010	324	0,1938	0,0002	0,512563	0,000002							f
Allende (ter)	CV3	980	313	0,1929	0,0002	0,512558	0,000003							f
Allende	CV3	854	275	0,1947		0,512566	0,000001							g
Allende	CV3							46,0	192	0,0341	0,0004	0,282835	0,000036	i
Allende (bis)	CV3							45,9	192	0,0341	0,0004	0,282795	0,000036	i
Allende (ter)	CV3							45,2	189	0,0340	0,0004	0,282839	0,000036	i
Allende (quarter)	CV3							48,5	206	0,0337	0,0004	0,282814	0,000036	i
Allende (quīnquiēs)	CV3							46,0	193	0,0340	0,0004	0,282824	0,000036	i
Allende (sexiēs)	CV3							46,4	193	0,0343	0,0004	0,282795	0,000036	i
Allende (septiēns)	CV3							46,1	192	0,0342	0,0004	0,282801	0,000036	i

Allende	CV3	735	241	0,1979		0,512670	0,000003							j
Allende	CV3	863	280	0,1959	0,0002	0,512651	0,000003							k
Allende (bis)	CV3	879	285	0,1961	0,0002	0,512664	0,000006							k
Allende (ter)	CV3	1009	325	0,1948	0,0002	0,512620	0,000005							k
Allende	CV3			0,1950	0,0020	0,512608	0,000019							l
Grosnaja	CV3	1076	360	0,2024		0,512841	0,000001							g
Grosnaja	CV3							39,1	162	0,0345	0,0004	0,282811	0,000036	i
Mokoia	CV3	766	249	0,1963		0,512639	0,000001							g
Vigarano	CV3	876	282	0,1951	0,0010	0,512609	0,000010	41,8	174	0,0340	0,0002	0,282811	0,000006	h
Vigarano	CV3							49,2	207	0,0338	0,0004	0,282789	0,000036	i
Ningqiang	CK3	1098	357	0,1965	0,0010	0,512639	0,000008	68,8	276	0,0353	0,0002	0,282947	0,000004	h
Karoonda	CK4	932	301	0,1951	0,0004	0,512602	0,000007	47,4	190	0,0354	0,0002	0,282951	0,000010	e
Qingzhen	EH3							24,5	107	0,0326	0,0004	0,282704	0,000036	i
Abee	EH4			0,2000	0,0002	0,512726	0,000022							b
Abee	EH4	464	146	0,1903	0,0002	0,512586	0,000008							f
Abee	EH4	229	71	0,1874	0,0002	0,512395	0,000006							k
Abee (bis)	EH4	278	88	0,1903	0,0002	0,512490	0,000005							k
Adhi Kot	EH4							23,9	73,3	0,0465	0,0004	0,284055	0,000036	i
Indarch	EH4	412	133	0,1957	0,0004	0,512603	0,000006	24,8	105	0,0335	0,0002	0,282797	0,000009	e
Indarch	EH4	365	117	0,1934		0,512623	0,000001							g
Indarch	EH4							23,5	104	0,0320	0,0004	0,282685	0,000036	i
Indarch	EH4	440	142	0,1953	0,0002	0,512622	0,000006							k
Indarch (bis)	EH4	439	141	0,1948	0,0002	0,512611	0,000005							k
St. Mark's	EH5							23,2	87,7	0,0377	0,0004	0,283143	0,000036	i
St. Mark's	EH5	452	146	0,1953		0,512604	0,000002							j
Saint-Sauveur	EH5							20,3	76,1	0,0381	0,0004	0,283250	0,000036	i
Saint-Sauveur	EH5	458	148	0,1956	0,0002	0,512624	0,000003							k
Daniel’s Kuil	EL6							29,3	138	0,0302	0,0004	0,282528	0,000036	i
Eagle	EL6							31,2	176	0,0252	0,0004	0,281972	0,000036	i

Hvittis	EL6							30,4	134	0,0322	0,0004	0,282651	0,000036	i
Hvittis	EL6	361	120	0,2007		0,512750	0,000003							j
Hvittis	EL6	480	159	0,1999	0,0002	0,512758	0,000003							k
Hvittis (bis)	EL6	818	269	0,1986	0,0002	0,512753	0,000006							k
Hvittis (ter)	EL6	557	183	0,1993	0,0002	0,512766	0,000005							k
Jajh Deh Kot Lalu	EL6							22,9	159	0,0205	0,0004	0,281675	0,000036	i
Khairpur	EL6							24,1	137	0,0250	0,0004	0,282061	0,000036	i
Khairpur	EL6	411	134	0,1965		0,512633	0,000002							j
Pillistfer	EL6							26,8	119	0,0320	0,0003	0,282708	0,000014	c
Pillistfer	EL6							25,0	113	0,0316	0,0004	0,282648	0,000036	i
Chondrite fall mean				**0,1955**	**0,0005**	**0,512622**	**0,000012**			**0,0331**	**0,0006**	**0,282757**	**0,000056**	
***N* for the mean values**					***107***							***96***		
Antarctic chondrites														
GRA 95229 (WI: A)	CR2							44,6	188	0,0336	0,0002	0,282787	0,000007	h
ALHA 77295 (WI: B)	EH3	344	114	0,2009		0,512607	0,000003							j
KLE 98300 (WI: A)	EH3	490	160	0,1976	0,0010	0,512668	0,000007	24,0	124	0,0273	0,0001	0,282208	0,000004	h
MAC 88136 (WI: A)*	EL3	397	127	0,1936	0,0010	0,512553	0,000008	29,0	122	0,0338	0,0002	0,282794	0,000007	h
MAC 88180 (WI: C)*	EL3	819	267	0,1974		0,512732	0,000003							j
MAC 02837 (WI: C)	EL3	497	163	0,1987		0,512653	0,000000							j
MAC 02839 (WI: C)	EL3	572	187	0,1976		0,512642	0,000003							j
Antarctic chondrite mean				**0,1976**	**0,0019**	**0,512643**	**0,000049**			**0,0316**	**0,0043**	**0,282596**	**0,000388**	
***N* for the mean values**					***6***							***3***		

The weathering indexes for Antarctic chondrites are from Antarctic Meteorite Newsletter, NASA. The chondrite fall mean includes H chondrite falls.

*MAC 88136 and MAC 88180 are possibly paired (Antarctic Meteorite Newsletter 13, NASA).

[a] Jacobsen and Wasserburg (1980). [b] Jacobsen and Wasserburg (1984). [c] Blichert-Toft and Albarède (1997). [d] Bizzarro *et al*. (2003). [e] Patchett *et al*. (2004). [f] Boyet and Carlson (2005). [g] Carlson *et al*. (2007). [h] Bouvier *et al*. (2008). [i] Dauphas and Pourmand (2011). [j] Gannoun *et al*. (2011). [k] Burkhardt *et al*. (2016). [l] Fukai and Yokoyama (2017).